



7N-34  
197739  
438

# TECHNICAL NOTE

## D-207

HYDRODYNAMIC IMPACT-LOADS INVESTIGATION  
OF CHINE-IMMERSED  $0^\circ$  DEAD-RISE CONFIGURATIONS HAVING  
LONGITUDINAL CURVATURE

WITH AN APPENDED BIBLIOGRAPHY OF  
LANGLEY IMPACT BASIN HYDRODYNAMIC PUBLICATIONS

By Robert W. Miller

Langley Research Center  
Langley Field, Va.

NATIONAL AERONAUTICS AND SPACE ADMINISTRATION  
WASHINGTON

February 1960

(NASA-TN-D-207) HYDRODYNAMIC IMPACT-LOADS  
INVESTIGATION OF CHINE-IMMERSED 0 DEGREE  
DEAD-RISE CONFIGURATIONS HAVING LONGITUDINAL  
CURVATURE WITH AN APPENDED BIBLIOGRAPHY OF  
LANGLEY IMPACT BASIN HYDRODYNAMIC (NASA.

N89-70759

Unclass

00/34 0197739

## NATIONAL AERONAUTICS AND SPACE ADMINISTRATION

## TECHNICAL NOTE D-207

HYDRODYNAMIC IMPACT-LOADS INVESTIGATION  
OF CHINE-IMMERSED  $0^\circ$  DEAD-RISE CONFIGURATIONS HAVING  
LONGITUDINAL CURVATUREWITH AN APPENDED BIBLIOGRAPHY OF  
LANGLEY IMPACT BASIN HYDRODYNAMIC PUBLICATIONS

By Robert W. Miller

## SUMMARY

To investigate the relationship of bottom configuration to hydrodynamic impact loads, tests were made of two  $0^\circ$  dead-rise, narrow-beam configurations; one having the forward half curved upward, the other having the same curvature over the rear half. The tests were made in smooth water over a range of flight-path angles at several fixed trim angles with beam-loading coefficients of about 18, 29, and 36.

The load, motion, and moment data obtained at impact from both configurations and the maximum-pressure data for the curved-stern configuration are presented in tabular form. The results are plotted in coefficient form, and some typical time histories are also presented. The trends of the coefficients with initial flight-path angle, trim, and beam loading for both configurations are generally similar to those exhibited by other chine-immersed models. Comparison of the results for the two configurations at positive trims revealed no significant differences due to longitudinal curvature, but comparison at  $0^\circ$  trim indicated load alleviation by the curved stern.

The present investigation is the last of a program on impact loads on narrow-beam models and also the last to be reported from the recently deactivated Langley impact basin. The opportunity is therefore taken to include a bibliography of all other publications on hydrodynamic programs from this basin.

## INTRODUCTION

In the design of water-based aircraft a basic problem has been that of obtaining hydrodynamic configurations with low landing-impact loads. The fundamentals of impact loads as related to seaplane body configuration were investigated for several years at the Langley impact basin.

These investigations have generally dealt with experimental studies of impact loads on basic shapes of models. From the standpoint of impact loads these tests can be grouped as wide-beam configurations (non-chine immersed) or as narrow-beam configurations (chine immersed). The data obtained on these basic configurations can be applied to the design of specific seaplane hulls or hydro-skis. The investigation with which this paper is concerned concludes the program at the Langley impact basin on narrow-beam configurations. Also, since this research facility has now been deactivated, this opportunity is taken to present a bibliography of the publications of other hydrodynamic research programs carried out at the Langley impact basin. For convenience, this bibliography is subdivided according to subject matter.

The data of the present investigation deal with the hydrodynamic impact loads on a chine-immersed  $0^\circ$  dead-rise model having longitudinal curvature. This investigation was part of a program dealing primarily with effects of transverse shape but included a few investigations to determine some of the effects of longitudinal curvature on impact loads. Among the configurations tested with longitudinal curvature were a concave-convex shape (ref. 1), a  $30^\circ$  dead-rise V-shape (ref. 2), and the flat-bottom model used for the present investigation.

This investigation is concerned with the loads and motions of two  $0^\circ$  dead-rise, narrow-beam configurations: one having the forward half curved upward, the other having the same curvature over the rear half. The tests consisted of a series of impacts in smooth water for a range of flight-path angles at several fixed trims. Most of the runs were made at a beam-loading coefficient of about 18 but a few runs were made at loading coefficients of 29 and 36.

The data presented in this paper include load, motion, and moment data obtained at impact from both configurations, and maximum pressure data for the curved-stern configuration. The load, motion, and moment data are presented tabularly and are plotted in coefficient form, and some typical time histories are also presented. Load, motion, moment, and time coefficients for the two configurations at two of the trims are presented in such a manner that the parameters are fixed except for the shape and initial flight-path angle against which they are plotted. These plots provide direct comparisons of some of the effects of longitudinal curvature.

#### SYMBOLS

b            model beam, ft

$F_v$         hydrodynamic force normal to undisturbed water surface, lb

L  
2  
7  
0

$g$	acceleration due to gravity, 32.2 ft/sec <sup>2</sup>
$M_Y$	pitching moment referred to stern, lb-ft
$n_i$	impact load factor, $F_v/W$
$p$	water pressure, lb/sq in.
$t$	time after water contact, sec
$V$	resultant velocity of model, fps
$W$	dropping weight, lb
$\dot{x}$	velocity of model parallel to undisturbed water surface, fps
$z$	model draft, ft
$\dot{z}$	vertical velocity of model, fps
$\gamma$	flight-path angle relative to undisturbed water surface, deg
$\rho$	mass density of water, 1.938 slugs/cu ft
$\tau$	trim angle (angle between tangent to the keel at stern and undisturbed water surface), deg

Dimensionless variables:

$C_d$	draft coefficient, $z/b$
$C_v$	vertical-velocity coefficient, $\dot{z}/\dot{z}_0$
$C_L$	impact lift coefficient, $\frac{F_v}{\frac{1}{2}\rho b^2 V_o^2}$
$C_m$	pitching-moment coefficient, $\frac{M_Y}{\frac{1}{2}\rho b^3 V_o^2}$
$C_{cp}$	center-of-pressure coefficient, center-of-pressure distance from stern-keel point in beams
$C_t$	time coefficient, $\frac{V_o t}{b}$

$C_{\Delta}$  beam-loading coefficient,  $\frac{W}{\rho g b^3}$

Subscripts:

o instant of initial contact with water surface

max maximum

## APPARATUS AND TEST PROCEDURE

### Basin and Models

The tests were made in the Langley impact basin with the equipment described in reference 3. This equipment consisted of a catapult, an arresting gear, a testing carriage to which the model was attached, and instrumentation for measuring the loads and motions of the model. The model was attached to the carriage at all times by a boom mounted on a parallel linkage which permitted the model to have the forward motion of the carriage and a free vertical motion while restrained in pitch, roll, and yaw.

A profile view showing pertinent dimensions of the model is shown in figure 1. The model was 10 feet in length and had a 1-foot beam. It was basically of sheet-metal construction and was designed so that any deflection under load could be considered negligible. The chines were sharp enough to insure flow separation, and the parts of the model above the chines, therefore, had no effect on the test results. The bottom was flat in transverse cross section but longitudinally one-half was flat and the other half was curved upward on a 120-inch radius. The attachment points were arranged so that either end could be used as the stern. Figure 2(a) shows the model in testing position as a curved-bow configuration at  $0^\circ$  trim and figure 2(b) shows it as a curved-stern configuration at  $0^\circ$  trim.

### Instrumentation and Accuracy

The instruments consisted of accelerometers, a dynamometer, a water-contact indicator, and electrical pickups for measuring displacements, velocities, and hydrodynamic pressure. The data from these instruments were recorded on a multichannel oscillograph along with 0.01-second timing.

Accelerations were measured in the vertical direction by an unbonded strain-gage-type accelerometer having a range of  $\pm 6g$  and a natural frequency of 17 cycles per second. Pitching moments about the step were

obtained from a strain-gage-type dynamometer mounted between the model and the carriage boom. The measured moments were adjusted for the effect of the mass below the dynamometer and transferred to the step. Model contact with the water was indicated by an electric circuit completed by the water. Horizontal and vertical displacements were obtained from a photoelectric cell and slide-wire, respectively, as described in reference 3. Vertical velocity of the model was determined by means of a generator driven by the vertical movement of the carriage boom. The pressures were measured by 12 induction-type gages which had 1/2-inch-diameter diaphragms mounted flush with the model bottom and were distributed along the center line as shown in figure 3.

The apparatus used in these tests yields measurements that are believed correct within the following limits:

Horizontal velocity, ft/sec . . . . .	±0.5
Vertical velocity, ft/sec . . . . .	±0.2
Draft, ft . . . . .	±0.03
Acceleration, g units . . . . .	±0.2
Weight, lb . . . . .	±10.0
Pitching moment, percent . . . . .	±8.0
Pressure, percent . . . . .	±10.0
Time, sec . . . . .	±0.002

#### Test Conditions

A summary of the test conditions for both configurations is presented in table I.

The curved-bow configuration was tested at fixed trim angles of  $-3^{\circ}$  to  $23^{\circ}$ . The horizontal velocity at contact was varied from approximately 20 to 72 feet per second, and the vertical velocity at contact varied from approximately 2 to 13 feet per second. These velocities resulted in a range of flight-path angles at water contact of  $2.5^{\circ}$  to  $22.8^{\circ}$ . Dropping weights of about 1,150, 1,807, and 2,264 pounds gave beam-loading coefficients  $C_{\Delta}$  of about 18.4, 29.0, and 36.3, respectively.

The curved-stern configuration was tested at fixed trim angles (tangent to the bottom at the stern with respect to undisturbed water) of  $16^{\circ}$  to  $-22^{\circ}$ . The horizontal velocity at contact was varied from approximately 33 to 90 feet per second and the vertical velocity at contact varied from approximately 5 to 13 feet per second. These velocities resulted in flight-path angles at water contact of  $3.2^{\circ}$  to  $20.7^{\circ}$ . Dropping weights of about 1,147 and 2,264 pounds gave  $C_{\Delta}$  values of 18.4 and 36.3, respectively.

## RESULTS AND DISCUSSION

The primary purpose of this investigation was to extend studies of impact loads on chine-immersed flat-bottom (zero dead-rise) bodies with upward-curved bow or upward-curved stern. The data and results presented are also of interest in the consideration of the general problem of loads on narrow-beam models. In the following paragraphs, a brief discussion of the behavior of each model is presented, together with some effects of longitudinal curvature observed in these tests.

The experimental data were obtained from the tests as time histories of draft, vertical velocity, vertical acceleration, pitching moment, and hydrodynamic bottom pressure. The values of the initial conditions and the recorded motion, load, and moment data at maximum acceleration, maximum draft, and rebound are given in table II. The data for both configurations are given in this table, the first 96 runs being for the curved-bow configuration and the other 72 for the curved-stern configuration. The maximum pressure recorded on each gage and the time after contact at which this pressure occurred are given in table III for the curved-stern configuration. The initial conditions for each run are also repeated for convenience.

Time histories of the coefficients of draft, vertical velocity, hydrodynamic lift, pitching moment about the step, and center of pressure from contact to the time of maximum draft are presented in figure 4 for three typical runs. These time histories give an overall picture of the sequence of events during the runs. They were chosen to illustrate the effect on the results of varying certain test conditions.

Figures 4(a) and 4(b) represent for the curved-bow configuration the effect of increasing trim while maintaining other parameters approximately constant. It can be noted from these plots that as trim increases, although the maximum draft coefficient  $C_d$  remains almost constant, the maximum impact-lift coefficient  $C_L$  is reduced but the lift coefficient is maintained for a longer period and the moment and center-of-pressure coefficients are reduced. Figures 4(a) and 4(c) show that for the low trim condition, the curved stern considerably reduced the maximum lift and moment coefficients and caused the center of pressure to remain near the stern. Actually, the results for the curved-stern configuration at  $0^\circ$  trim (fig. 4(c)) resemble the results for the curved-bow configuration at  $23^\circ$  trim (fig. 4(b)). It should be noted, however, that at high trims the curved bow does not become immersed and, therefore, this configuration is essentially a straight-keel configuration.

As a means of analyzing the results, the data given in table II were converted into dimensionless coefficient form. In this manner the results

obtained for each impact can be compared with results of all the other impacts, with trim and flight-path angle being the only variables for a given shape and beam-loading condition. The draft coefficients at the instants of maximum draft and maximum acceleration, the vertical-velocity coefficients at maximum acceleration and at rebound, the maximum impact-lift coefficient, the pitching-moment and center-of-pressure coefficients at the instant of maximum acceleration, and the time coefficients at maximum acceleration, maximum draft, and rebound were computed from the experimental data. These experimental coefficients were then plotted in figures 5, 6, 7, 8, 9, and 10 against initial flight-path angle for each trim and beam-loading coefficient.

In figure 5 the trend of draft coefficient with initial flight-path angle at each tested trim and beam loading can be directly observed from the plots. The trends with trim and with beam loading can be observed by comparing the plots for a given configuration with each other, and effects of longitudinal curvature can be observed by comparing the plots of figure 5(a) with those of figure 5(b). It should be noted that for the curved-bow configuration (fig. 5(a)) a line is drawn on the positive trim plots indicating the draft coefficient at which geometric bow immersion begins. The positions of these lines indicate that for trims above  $3^\circ$ , the bow was not immersed at the time of maximum acceleration, and these data can be considered essentially straight-keel data. However, for the lower trim data and most of the maximum-draft data at the intermediate trims, the bow was immersed for at least a part of the impact.

The trends of vertical velocity, maximum-impact lift, pitching moment, center-of-pressure, and time coefficients with initial flight-path angle, trim, and beam-loading coefficient can be observed in figures 6, 7, 8, 9, and 10, respectively, in a manner similar to that described for the draft coefficient in figure 5. Likewise, some effects of longitudinal curvature can be observed by comparing the (a) and (b) parts of each figure. The trends of the coefficients with initial flight-path angle, trim, and beam loading are in general similar to those described in references 1 and 2 and will not all be discussed individually.

In order to compare more directly the effects of longitudinal curvature, figure 11 presents curves of the draft, vertical-velocity, impact-lift, pitching-moment, center-of-pressure, and time coefficients obtained by fairing the data as presented in figures 5, 6, 7, 8, 9, and 10 at a draft coefficient of 18 for  $8^\circ$  and  $0^\circ$  of trim. In this manner the parameters have been fixed except for the shape of the configuration and the initial flight-path angle, against which the coefficients are plotted.

From the comparison at  $8^\circ$  trim (fig. 11(a)) no large differences between the results for the two configurations are apparent. The curved-stern configuration went only slightly deeper into the water than the



curved-bow configuration at both maximum load and maximum draft. The trends of the vertical velocities at both maximum load and exit are similar. The maximum lift, moment, and center-of-pressure coefficients indicate no significant differences for the configurations. Among the time coefficients the only appreciable difference is that at exit which shows that the curved-stern configuration leaves the water in a considerably shorter time than the curved-bow configuration.

In the  $0^\circ$  trim case (fig. 11(b)) the curved-stern configuration attains considerably greater drafts than the curved-bow configuration, especially at maximum load which the curved-bow configuration attains at very shallow drafts. The curved-bow configuration has quite high vertical velocities at maximum load and very small vertical velocities at exit, while the curved-stern configuration does not show much change from the  $8^\circ$  trim condition. The curved-stern configuration has much lower values of maximum lift, moment, and center of pressure than the curved-bow configuration. From the time coefficient plot can be seen that the curved-bow configuration attains maximum load almost instantly on contact and requires less time to exit at high flight-path angles than at low ones; while the curved-stern configuration has the opposite trend.

Thus, the comparison of the two configurations at  $0^\circ$  trim shows considerable difference in the results. The curved-bow configuration, which has a large flat area involved immediately on contact at this attitude, shows a much larger and more rapid buildup of load than the curved-stern configuration. Thus, the stern curvature can be looked upon, in this instance, as a load-relieving device which by spreading the impact over more time and a deeper immersion attains a reduction of the maximum loads and moments. This effect could be of importance in rough-water landings where low-trim, high effective flight-path angle impacts that produce large loads are common.

#### CONCLUDING REMARKS

Hydrodynamic impact tests were made in the Langley impact basin using two  $0^\circ$  dead-rise, narrow-beam configurations; one having longitudinal upward curvature over the forward half, the other having the same curvature over the rear half. The tests were made in smooth water for a range of flight-path angles at several fixed trims with beam loading coefficients of about 18, 29, and 36.

The trends of the coefficients with initial flight-path angle, trim, and beam loading, for both configurations are generally similar to those exhibited by other chine-immersed models.

Comparisons between the results for the two configurations at positive trims have revealed only small differences in behavior due to longitudinal curvature. However, comparison at  $0^\circ$  trim shows that the curved-bow configuration, which has a large flat area involved immediately on contact at this attitude, has a large rapid buildup of load and moment. On the other hand, the curved-stern configuration, which spreads the impact over more time and a deeper immersion, attains a considerable reduction of the maximum loads and moments. This reduction of loads and moments could be of importance in rough-water landings, where low trim, high effective flight-path-angle impacts are common.

Langley Research Center,  
National Aeronautics and Space Administration,  
Langley Field, Va., October 23, 1959.

#### REFERENCES

1. Edge, Philip M., Jr.: Impact-Loads Investigation of Chine-Immersed Models Having Concave-Convex Transverse Shape and Straight or Curved Keel Lines. NACA TN 3940, 1957.
2. Edge, Philip M., Jr., and Mixson, John S.: Impact-Loads Investigation of a Chine-Immersed Model Having a Longitudinally Curved Bow and a V-Bottom With a Dead-Rise Angle of  $30^\circ$ . NACA TN 4106, 1957.
3. Batterson, Sidney A.: The NACA Impact Basin and Water Landing Tests of a Float Model at Various Velocities and Weights. NACA Rep 795, 1944. (Supersedes NACA WR L-163.)

## BIBLIOGRAPHY OF LANGLEY IMPACT BASIN

## HYDRODYNAMIC PUBLICATIONS

## Theory

- Markey, Melvin F.: A Generalized Hydrodynamic-Impact Theory for the Loads and Motions of Deeply Immersed Prismatic Bodies. NASA MEMO 2-10-59L, 1959.
- Mayo, Wilbur L.: Analysis and Modification of Theory for Impact of Seaplanes on Water. NACA Rep. 810, 1945. (Supersedes NACA TN 1008.)
- Mayo, Wilbur L.: Hydrodynamic Impact of a System With a Single Elastic Mode. I - Theory and Generalized Solution With an Application to an Elastic Airframe. NACA Rep. 1074, 1952. (Supersedes NACA TN 1398.)
- Miller, Robert W.: Comparison of Hydrodynamic-Impact Accelerations and Response for Systems With Single and With Multiple Elastic Modes. NACA TN 4194, 1958.
- Miller, Robert W.: Theoretical Analysis of Hydrodynamic Impact of a Prismatic Float Having Freedom in Trim. NACA TN 2698, 1952.
- Miller, Robert W., and Merten, Kenneth F.: Hydrodynamic Impact of a System With a Single Elastic Mode. II - Comparison of Experimental Force and Response With Theory. NACA Rep. 1075, 1952. (Supersedes NACA TN 2343.)
- Milwitzky, Benjamin: A Theoretical Investigation of Hydrodynamic Impact Loads on Scalloped-Bottom Seaplanes and Comparisons With Experiment. NACA Rep. 867, 1947. (Supersedes NACA TN 1363.)
- Milwitzky, Benjamin: A Generalized Theoretical and Experimental Investigation of the Motions and Hydrodynamic Loads Experienced by V-Bottom Seaplanes During Step-Landing Impacts. NACA TN 1516, 1948.
- Milwitzky, Benjamin: A Generalized Theoretical Investigation of the Hydrodynamic Pitching Moments Experienced by V-Bottom Seaplanes During Step-Landing Impacts and Comparisons With Experiment. NACA TN 1630, 1948.
- Milwitzky, Benjamin: Generalized Theory for Seaplane Impact. NACA Rep. 1103, 1952.

L  
2  
7  
0

Schnitzer, Emanuel: Theory and Procedure for Determining Loads and Motions in Chine-Immersed Hydrodynamic Impacts of Prismatic Bodies. NACA Rep. 1152, 1953. (Supersedes NACA TN 2813.)

Schnitzer, Emanuel, and Hathaway, Melvin F.: Estimation of Hydrodynamic Impact Loads and Pressure Distributions on Bodies Approximating Elliptical Cylinders With Special Reference to Water Landings of Helicopters. NACA TN 2889, 1953.

Schnitzer, Emanuel: Estimation of Water Landing Loads on Hydro-Ski-Equipped Aircraft. NACA RM L53D29, 1953.

Schnitzer, Emanuel: Water-Impact Theory for Aircraft Equipped With Nontrimming Hydro-Skis Mounted on Shock Struts. NACA TN 4256, 1958. (Supersedes NACA RM L54H10.)

Schnitzer, Emanuel: Reduction of Hydrodynamic Impact Loads for Waterborne Aircraft. NACA RM L55E09b, 1955.

Schnitzer, Emanuel: Theoretical Determination of Water Loads on Pitching Hulls and Shock-Mounted Hydro-Skis. NACA RM L56E31, 1956.

Sims, Joseph L., and Schnitzer, Emanuel: A Theoretical Investigation of the Effect of Partial Wing Lift on Hydrodynamic Landing Characteristics of V-Bottom Seaplanes in Step Impacts. NACA TN 2815, 1952.

Smiley, Robert F.: A Semiempirical Procedure for Computing the Water-Pressure Distribution on Flat and V-Bottom Prismatic Surfaces During Impact or Planing. NACA TN 2583, 1951.

Smiley, Robert F.: The Application of Planing Characteristics to the Calculation of the Water-Landing Loads and Motions of Seaplanes of Arbitrary Constant Cross Section. NACA TN 2814, 1952.

Steiner, Margaret F.: Analysis of Planing Data for Use in Predicting Hydrodynamic Impact Loads. NACA TN 1694, 1948.

#### Flight Tests

Haines, Gilbert A.: Comparison of Pitching Moments Obtained During Seaplane Landings With Values Predicted by Hydrodynamic Impact Theory. NACA TN 1881, 1949.

Merten, Kenneth F., and Beck, Edgar B.: Effect of Wing Flexibility and Variable Air Lift upon Wing Bending Moments during Landing Impacts of a Small Seaplane. NACA Rep. 1013, 1951. (Supersedes NACA TN 2063 by Kenneth F. Merten, José L. Rodríguez, and Edgar B. Beck.)

Savitsky, Daniel: Theoretical and Experimental Wing-Tip Accelerations of a Small Flying Boat During Landing Impacts. NACA TN 1690, 1948.

Steiner, Margaret F.: Comparison of Over-All Impact Loads Obtained During Seaplane Landing Tests With Loads Predicted by Hydrodynamic Theory. NACA TN 1781, 1949.

#### Research Equipment and Techniques

Batterson, Sidney A.: The NACA Impact Basin and Water Loading Tests of a Float Model at Various Velocities and Weights. NACA Rep. 795, 1944. (Supersedes NACA WR L-163.)

L  
2  
7  
0

Edge, Philip M., Jr.: Instrumentation for Investigation of Seaplane Impact Loads in Waves. Proc. First Conf. on Coastal Eng. Instruments (Berkeley, Calif., Oct. 31 - Nov. 2, 1955), Council on Wave Res., The Eng. Foundation, 1956, pp. 213-226.

Markey, Melvin F.: Effect of Carriage Mass Upon the Loads and Motions of a Prismatic Body During Hydrodynamic Impact. NACA TN 3619, 1956.

#### Wide-Beam Configurations

Batterson, Sidney A.: Variation of Hydrodynamic Impact Loads With Flight-Path Angle for a Prismatic Float at  $3^\circ$  Trim and With a  $22\frac{1}{2}^\circ$  Angle of Dead Rise. NACA WR L-211, 1945. (Formerly NACA RB L5A24.)

Batterson, Sidney A.: Variation of Hydrodynamic Impact Loads With Flight-Path Angle for a Prismatic Float at  $12^\circ$  Trim and With a  $22\frac{1}{2}^\circ$  Angle of Dead Rise. NACA WR L-68, 1946. (Formerly NACA RB L5K21a.)

Batterson, Sidney A., and Stewart, Thelma: Variation of Hydrodynamic Impact Loads With Flight-Path Angle for a Prismatic Float at  $6^\circ$  and  $9^\circ$  Trim and a  $22\frac{1}{2}^\circ$  Angle of Dead Rise. NACA WR L-69, 1946. (Formerly NACA RB L5K21.)

Batterson, Sidney A.: Variation of Hydrodynamic Impact Loads With Flight-Path Angle for a Prismatic Float at  $0^\circ$  and  $-3^\circ$  Trim and With a  $22\frac{1}{2}^\circ$  Angle of Dead Rise. NACA TN 1166, 1947.

Edge, Philip M., Jr.: Hydrodynamic Impact Loads in Smooth Water for a Prismatic Float Having an Angle of Dead Rise of  $40^{\circ}$ . NACA TN 1775, 1949.

Edge, Philip M., Jr.: Hydrodynamic Impact Loads in Smooth Water for a Prismatic Float Having an Angle of Dead Rise of  $10^{\circ}$ . NACA TN 3608, 1956.

Mayo, Wilbur L.: Theoretical and Experimental Dynamic Loads for a Prismatic Float Having an Angle of Dead Rise of  $22\frac{1}{2}^{\circ}$ . NACA WR L-70, 1945. (Formerly NACA RB L5F15.)

Miller, Robert W.: Hydrodynamic Impact Loads in Rough Water for a Prismatic Float Having an Angle of Dead Rise of  $30^{\circ}$ . NACA TN 1776, 1948.

Miller, Robert W., and Leshnover, Samuel: Hydrodynamic Impact Loads in Smooth Water for a Prismatic Float Having an Angle of Dead Rise of  $30^{\circ}$ . NACA TN 1325, 1947.

Smiley, Robert F.: Water-Pressure Distributions During Landings of a Prismatic Model Having an Angle of Dead Rise of  $22\frac{1}{2}^{\circ}$  and Beam-Loading Coefficients of 0.48 and 0.97. NACA TN 2816, 1952.

Smiley, Robert F.: A Theoretical and Experimental Investigation of the Effects of Yaw on Pressures, Forces, and Moments During Seaplane Landings and Planing. NACA TN 2817, 1952.

#### Narrow-Beam Configurations

Batterson, Sidney A., and McArver, A. Ethelda: Water Landing Investigation of a Model Having a Heavy Beam Loading and a  $30^{\circ}$  Angle of Dead Rise. NACA TN 2015, 1950.

Batterson, Sidney A.: Water Landing Investigation of a Hydro-Ski Model at Beam Loadings of 18.9 and 4.4. NACA RM L51F27, 1951.

Edge, Philip M., Jr.: Impact-Loads Investigation of Chine-Immersed Models Having Concave-Convex Transverse Shape and Straight or Curved Keel Lines. NACA TN 3940, 1957.

Edge, Philip M., Jr.: Impact-Loads Investigation of Chine-Immersed Model Having a Circular-Arc Transverse Shape. NACA TN 4103, 1957.

- Edge, Philip M., Jr., and Mixson, John S.: Impact-Loads Investigation of a Chine-Immersed Model Having a Longitudinally Curved Bow and a V-Bottom With a Dead-Rise Angle of  $30^{\circ}$ . NACA TN 4106, 1957.
- Edge, Philip M., Jr.: Hydrodynamic Impact Loads of a  $-20^{\circ}$  Dead-Rise Inverted-V Model and Comparisons With Loads of a Flat-Bottom Model. NACA TN 4339, 1958.
- Edge, Philip M., Jr., and Mason, Jean P.: Hydrodynamic Impact Loads on  $30^{\circ}$  and  $60^{\circ}$  V-Step Plan-Form Models With and Without Dead Rise. NACA TN 4401, 1958.
- Edge, Philip M., Jr.: Hydrodynamic Impact-Load Alleviation With a Penetrating Hydro-Ski. NASA MEMO 1-9-59L, 1959.
- Markey, Melvin F., and Carpini, Thomas D.: Rough-Water Impact-Load Investigation of a Chine-Immersed V-Bottom Model Having a Dead-Rise Angle of  $10^{\circ}$ . NACA TN 4123, 1957.
- McArver, A. Ethelda: Water-Landing Investigation of a Model Having Heavy Beam Loadings and  $0^{\circ}$  Angle of Dead Rise. NACA TN 2330, 1951.
- Miller, Robert W.: Comparison of Experimental Hydrodynamic Impact Loads and Motions for a V-Step and a Transverse-Step Hydro-Ski. NACA RM L53K20a, 1954.
- Miller, Robert W.: Water-Landing Investigation of a Flat-Bottom V-Step Model and Comparison With a Theory Incorporating Planing Data. NACA TN 2932, 1953.
- Miller, Robert W.: Hydrodynamic Impact-Loads Investigation of Chine-Immersed  $0^{\circ}$  Dead-Rise Configurations Having Longitudinal Curvature With an Appended Bibliography of Langley Impact Basin Hydrodynamic Publications. NASA TN D-207, 1959.
- Mixson, John S.: The Effect of Beam Loading on Water Impact Loads and Motions. NASA MEMO 1-5-59L, 1959.
- Smiley, Robert F.: A Study of Water Pressure Distributions During Landings With Special Reference to a Prismatic Model Having a Heavy Beam Loading and a  $30^{\circ}$  Angle of Dead Rise. NACA TN 2111, 1950.
- Smiley, Robert F.: An Experimental Study of Water-Pressure Distributions During Landings and Planing of a Heavily Loaded Rectangular Flat-Plate Model. NACA TN 2453, 1951.

TABLE I.- SUMMARY OF TEST CONDITIONS

Beam-loading coefficient, $C_{\Delta}$	Weight, $W$ , lb	Trim angle, $\tau$ , deg	Initial-flight-path angle, $\gamma_0$ , deg	Velocity range, $V_0$ , fps	Number of runs
Curved-bow configuration					
18.30	1,142	-3, 0, 3, 8, 13, 23	2.5 to 22.7	19 to 68	39
18.59	1,161	3, 8, 13, 23	3.7 to 22.8	31 to 69	34
28.96	1,807	8	4.1 to 21.9	22 to 70	9
36.28	2,264	8	3.0 to 21.5	23 to 72	14
Curved-stern configuration					
18.38	1,147	16, 8, 0, -8, -14, -22	3.2 to 20.7	33 to 90	68
36.28	2,264	0	3.5 to 19.2	36 to 87	4



TABLE II.- IMPACT TEST DATA

(a) Curved-bow configuration

Run	C <sub>Δ</sub>	At contact				At n <sub>i</sub> <sup>max</sup>					At z <sub>max</sub>		At rebound	
		$\dot{x}_0$ , fps	$\dot{z}_0$ , fps	V <sub>0</sub> , fps	γ <sub>0</sub> , deg	t, sec	n <sub>i</sub>	z, ft	$\dot{z}$ , fps	M <sub>y</sub> , lb-ft	t, sec	z, ft	t, sec	$\dot{z}$ , fps
τ = -3°														
1	18.3	47.2	3.0	47.3	3.70	0.144	0.4	0.30	1.0	3,700	0.248	0.34	0.708	-0.6
2	18.3	43.9	4.1	44.1	5.38	.108	.4	.32	2.5	3,893	.278	.49	.779	-.6
3	18.3	38.5	5.6	38.9	8.30	.035	.8	.17	5.0	5,396	.288	.69	.889	-1.0
4	18.3	34.0	6.4	34.6	10.72	.034	1.0	.16	5.5	6,197	.317	.82	1.127	-.4
τ = 0°														
5	18.3	47.2	2.6	47.2	3.21	0.028	0.4	0.06	2.3	1,672	0.246	0.27	0.786	-.2
6	18.3	42.6	3.9	42.7	5.26	.010	.5	.04	3.8	2,031	.276	.42	-----	-----
7	18.3	38.6	5.9	39.1	8.72	.026	1.3	.13	5.0	6,084	.292	.65	.551	-1.0
8	18.3	33.6	5.7	34.0	9.57	.026	1.2	.12	4.8	5,319	.322	.67	-----	-----
τ = 3°														
9	18.3	45.3	2.0	45.3	2.52	0.042	0.3	0.07	1.7	486	0.272	0.22	-----	-----
10	18.3	65.1	3.2	65.2	2.85	.028	.6	.18	2.5	1,721	.205	.30	.626	-.8
11	18.3	53.8	2.8	53.9	2.98	.064	.5	.15	2.0	1,046	.234	.28	.731	-.5
12	18.3	54.9	2.9	55.0	2.98	.050	.5	.14	2.4	1,364	.230	.30	.814	-.6
13	18.3	55.9	3.0	56.0	3.08	.020	.5	.13	2.4	641	.220	.31	-----	-----
14	18.3	38.9	2.3	39.0	3.34	.052	.3	.11	1.9	1,024	.312	.28	-----	-----
15	18.3	55.6	3.4	55.7	3.43	.063	.6	.18	2.6	1,639	.243	.35	.768	-.7
16	18.3	56.0	3.4	56.1	3.51	.054	.6	.15	2.7	2,302	.234	.33	.680	-.4
17	18.3	47.6	3.0	47.7	3.56	.058	.5	.15	2.3	1,511	.283	.33	.928	-.4
18	18.3	55.8	3.5	55.9	3.57	.062	.6	.18	2.5	1,523	.220	.34	.710	-.8
19	18.6	51.6	3.4	51.7	3.74	.073	.6	.20	2.3	1,106	.236	.34	.792	-.5
20	18.6	52.9	3.5	53.0	3.78	.049	.5	.14	2.8	355	.229	.32	.847	-.3
21	18.6	69.0	9.0	69.6	7.45	.043	2.3	.32	6.6	5,483	.193	.63	.573	-1.3
22	18.6	66.0	9.2	66.7	7.98	.044	2.3	.32	6.8	6,004	.193	.63	.595	-1.9
23	18.3	38.5	5.8	38.9	8.49	.055	1.0	.22	5.2	2,887	.317	.75	-----	-----
24	18.6	53.5	10.8	54.6	11.37	.042	2.7	.40	8.0	8,170	.212	.84	.731	-1.8
25	18.6	52.9	11.1	54.1	11.89	.030	2.6	.35	8.7	7,530	.223	.88	.738	-1.8
26	18.3	28.2	6.9	29.0	13.81	.026	1.1	.18	6.5	3,185	.385	.97	-----	-----
27	18.6	41.3	11.2	42.8	15.11	.041	2.6	.39	8.9	7,223	.283	1.71	.982	-1.2
28	18.6	40.2	11.4	41.8	15.47	.041	2.5	.34	9.2	7,562	.273	1.23	.955	-1.4
29	18.6	31.9	11.1	33.8	19.24	.044	2.4	.45	9.7	6,465	.322	1.37	-----	-----
30	18.6	32.3	12.3	34.6	20.84	.042	2.6	.43	9.6	7,648	.320	1.28	-----	-----
31	18.6	32.0	12.3	34.2	21.06	.044	2.8	.44	9.6	8,773	.341	1.31	-----	-----
32	18.3	19.8	8.3	21.5	22.67	.030	1.3	.30	6.9	4,680	.430	1.27	1.246	-1.2
33	18.6	32.2	12.2	34.4	22.84	.041	2.7	.46	9.7	8,360	.320	1.32	-----	-----
τ = 8°														
34	18.3	51.8	2.6	51.9	2.86	0.095	0.5	0.20	1.5	1,488	0.195	0.27	0.515	-1.2
35	18.3	68.0	3.5	68.1	2.95	.058	.9	.16	2.4	1,101	.138	.27	.331	-2.0
36	18.3	54.6	3.0	54.7	3.11	.080	.6	.11	2.8	1,020	.170	.26	.420	-1.4
37	18.3	64.5	7.0	64.9	6.23	.050	1.6	.32	5.2	2,982	.170	.55	.430	-3.1
38	18.6	67.6	9.2	68.2	7.74	.062	1.4	.36	5.8	3,470	.158	.54	.395	-3.8
39	18.6	65.4	9.3	66.0	8.21	.065	2.0	.45	6.0	4,473	.163	.66	.547	-3.9
40	18.3	37.6	5.4	38.0	8.25	.060	.7	.30	4.2	1,538	.290	.60	.819	-1.5
41	18.3	38.9	5.8	39.3	8.41	.071	.8	.42	4.0	2,984	.254	.72	.855	-1.3
42	18.6	54.4	10.9	55.4	11.37	.058	2.2	.53	8.0	3,804	.198	.92	.585	-3.6
43	18.6	53.9	11.1	55.0	11.68	.053	2.1	.48	8.4	2,683	.202	.90	.609	-3.3
44	18.3	26.5	7.0	27.4	14.88	.058	.9	.41	6.1	2,371	.378	1.10	-----	-----
45	18.6	42.4	11.7	44.0	15.44	.058	2.1	.55	8.6	3,985	.260	1.10	.822	-2.6
46	18.6	41.5	11.5	43.1	15.54	.062	2.0	.58	8.4	3,555	.251	1.13	.830	-2.7
47	18.3	21.1	7.6	22.4	19.93	.057	1.1	.48	6.1	3,722	.427	1.46	-----	-----
48	18.6	33.4	12.4	35.6	20.27	.061	2.0	.64	9.3	4,577	.316	1.43	1.108	-1.9
49	18.6	33.2	12.4	35.4	20.45	.071	1.9	.61	9.3	4,056	.322	1.41	1.079	-2.0
50	18.6	33.1	12.4	35.4	20.59	.058	2.0	.61	9.5	3,785	.300	1.38	1.116	-1.8
51	18.6	32.0	12.3	34.2	21.06	.059	1.9	.59	9.1	4,782	.306	1.34	1.147	-1.8

TABLE II.- IMPACT TEST DATA - Continued

(a) Curved-bow configuration - Concluded

Run	$C_{\Delta}$	At contact				At $n_{i\max}$					At $z_{\max}$		At rebound	
		$\dot{x}_O$ , fps	$\dot{z}_O$ , fps	$V_O$ , fps	$\gamma_O$ , deg	t, sec	$n_i$	z, ft	$\dot{z}$ , fps	$M_Y$ , lb-ft	t, sec	z, ft	t, sec	$\dot{z}$ , fps
$\tau = 13^\circ$														
52	18.3	45.7	3.1	45.8	3.93	0.098	0.6	0.24	2.0	1,118	0.194	0.30	0.442	-1.7
53	18.6	67.8	9.7	68.5	8.18	.069	2.4	.48	5.7	2,514	.141	.63	.354	-5.0
54	18.6	65.6	9.4	66.2	8.18	.074	2.4	.55	5.2	2,901	.135	.62	.470	-5.2
55	18.3	38.6	7.6	39.4	11.18	.080	1.2	.52	5.7	3,437	.240	.72	.678	-2.8
56	18.6	53.5	11.0	54.6	11.58	.070	2.2	.58	7.3	2,588	.183	.86	.477	-4.8
57	18.3	25.2	6.2	26.0	13.77	.101	.7	.53	4.5	2,182	.351	1.01	1.222	-.7
58	18.3	37.1	9.2	38.2	13.95	.070	1.5	.57	6.8	-----	.250	1.09	.757	-2.7
59	18.6	45.4	11.4	46.9	14.08	.072	2.1	.64	8.0	2,598	.215	1.03	.585	-4.4
60	18.6	41.1	10.8	42.5	14.73	.075	1.8	.64	7.3	2,538	.223	1.04	.650	-3.7
61	18.3	22.5	8.1	23.9	19.80	.069	.9	.53	6.9	2,840	.399	1.04	-----	-----
62	18.6	32.7	12.1	34.9	20.26	.078	1.7	.74	8.7	3,161	.288	1.39	.932	-2.9
63	18.6	32.3	12.1	34.4	20.53	.073	2.2	.70	9.0	2,975	.293	1.38	.929	-3.0
64	18.3	23.0	9.0	24.8	21.45	.078	1.1	.65	7.2	3,713	.388	1.50	1.404	-1.2
$\tau = 23^\circ$														
65	18.3	48.9	3.8	49.0	4.48	0.109	0.9	0.30	1.8	1,012	0.159	0.33	0.358	-2.8
66	18.6	64.7	9.5	65.4	8.32	.082	2.7	.52	4.0	2,410	.106	.56	.264	-6.6
67	18.3	40.0	6.3	40.5	8.89	.105	1.0	.53	4.0	1,850	.220	.72	.516	-3.6
68	18.6	53.5	10.9	54.6	11.49	.086	2.3	.65	6.0	2,068	.156	.80	.368	-6.5
69	18.3	29.1	8.0	30.2	15.46	.135	.9	.86	5.0	1,871	.310	1.21	.826	-3.1
70	18.6	40.6	10.8	42.0	16.81	.077	1.8	.73	6.8	2,273	.206	1.04	.531	-5.4
71	18.3	25.6	9.6	27.3	20.49	.124	1.0	.99	6.4	2,524	.350	1.55	1.024	-2.9
72	18.6	31.8	11.9	34.0	20.55	.109	1.6	.99	7.3	2,687	.268	1.42	.762	-4.3
73	18.6	31.6	12.1	33.8	21.02	.096	1.6	.91	8.3	2,565	.291	1.43	.802	-4.3
$\tau = 8^\circ$														
74	29.0	49.0	4.2	49.2	4.87	0.103	0.5	0.36	2.9	2,195	0.288	0.59	0.778	-1.6
75	29.0	56.2	5.4	56.4	5.44	.094	.5	.28	2.4	1,213	.224	.40	.572	-1.7
76	29.0	69.9	10.5	70.7	8.51	.075	1.8	.60	6.9	7,623	.214	.95	.564	-4.3
77	29.0	38.8	6.5	39.3	9.56	.093	.8	.53	4.7	4,864	.377	1.09	1.187	-1.3
78	29.0	58.5	11.3	59.6	10.95	.069	1.2	.60	8.1	8,930	.248	1.14	.667	-3.8
79	29.0	44.8	12.4	46.5	15.40	.069	1.8	.66	9.2	8,326	.312	1.48	.983	-2.7
80	29.0	22.1	8.3	23.6	20.49	.092	.8	.67	6.9	5,703	.466	1.62	1.630	-.7
81	29.0	33.0	12.8	35.4	21.12	.071	1.6	.70	9.9	8,387	.405	1.88	1.400	-1.7
82	29.0	31.8	12.8	34.2	21.88	.066	1.6	.72	10.0	8,252	.406	2.16	1.421	-4.7
83	36.3	61.5	3.2	61.6	2.96	.118	0.5	0.30	2.0	2,498	0.233	0.38	0.555	-2.0
84	36.3	55.2	3.2	55.3	3.33	.126	.4	.31	1.9	2,520	.261	.41	.643	-1.7
85	36.3	71.7	4.2	71.8	3.37	.118	.7	.33	2.4	3,595	.209	.42	.475	-2.3
86	36.3	68.5	4.3	68.6	3.60	.107	.6	.31	2.0	3,048	.207	.40	.492	-2.2
87	36.3	48.1	4.0	48.2	4.82	.110	.4	.37	2.7	2,557	.320	.61	.825	-1.8
88	36.3	40.7	5.9	41.2	8.20	.172	.6	.51	4.4	4,165	.450	1.01	1.132	-1.9
89	36.3	68.0	10.5	68.8	8.56	.064	1.7	.57	8.0	9,852	.238	1.09	.631	-4.6
90	36.3	58.5	11.2	59.5	10.84	.061	1.6	.62	9.0	10,203	.276	1.30	.776	-4.2
91	36.3	34.7	7.8	35.6	12.65	.090	.7	.62	6.2	5,489	.430	1.50	1.338	-1.7
92	36.3	44.0	11.5	45.5	14.68	.069	1.4	.72	9.3	9,098	.344	1.66	.972	-3.2
93	36.3	23.0	6.2	23.8	15.15	.144	.4	.74	4.6	3,699	.570	1.52	1.754	-1.0
94	36.3	32.7	10.8	33.4	18.29	.072	1.3	.76	10.6	9,207	.442	2.19	1.411	-2.6
95	36.3	23.6	8.3	25.3	19.11	.094	.7	.69	6.8	5,796	.554	1.97	1.654	-1.9
96	36.3	32.7	12.9	35.2	21.53	.068	1.4	.76	10.4	8,205	.462	2.29	1.478	-2.6

TABLE II.- IMPACT TEST DATA - Continued

(b) Curved-stern configuration

Run	C <sub>Δ</sub>	At contact				At n <sub>i</sub> max					At z <sub>max</sub>		At rebound	
		$\dot{x}_0$ , fps	$\dot{z}_0$ , fps	V <sub>0</sub> , fps	γ <sub>0</sub> , deg	t, sec	n <sub>i</sub>	z, ft	$\dot{z}$ , fps	M <sub>Y</sub> , lb-ft	t, sec	z, ft	t, sec	$\dot{z}$ , fps
τ = -22°														
97	18.4	89.3	5.0	89.4	3.24	0.070	1.1	0.29	3.3	8,058	0.157	0.40	0.418	-1.6
98	18.4	83.3	4.9	83.5	3.34	.071	1.2	.26	2.9	9,475	.143	.35	.377	-1.7
99	18.4	78.7	8.0	79.2	5.84	.073	1.7	.44	4.9	13,780	.168	.62	.462	-2.6
100	18.4	73.8	8.1	74.2	6.29	.057	1.7	.38	5.8	11,772	.177	.65	.494	-2.4
101	18.4	67.1	8.7	67.7	7.39	.058	1.6	.41	6.3	12,507	.192	.71	.657	-2.4
102	18.4	62.5	8.1	63.0	7.41	.063	1.5	.40	6.0	10,865	.212	.74	.648	-1.9
103	18.4	49.6	7.7	50.2	8.78	.056	1.1	.35	5.9	7,795	.266	.81	.894	-.8
104	18.4	46.7	8.1	47.4	9.83	.056	1.2	.37	6.4	8,253	.289	.89	.968	-1.4
105	18.4	54.0	9.9	55.0	10.40	.056	1.8	.45	7.5	12,777	.275	.96	.943	-1.8
τ = -14°														
106	18.4	85.1	4.9	85.2	3.31	0.080	1.4	0.30	2.7	8,542	0.124	0.35	0.284	-3.6
107	18.4	82.0	4.9	82.1	3.34	.080	1.1	.32	3.1	6,613	.152	.40	.417	-1.4
108	18.4	80.3	11.2	81.1	7.95	.061	2.6	.50	7.6	15,825	.147	.76	.359	-4.9
109	18.4	80.0	12.4	81.0	8.84	.054	2.8	.54	8.8	17,028	.151	.89	.402	-4.5
110	18.4	62.1	12.4	63.3	11.29	.027	2.5	.28	11.0	10,393	.185	.96	.502	-3.8
111	18.4	61.7	12.5	63.0	11.47	.025	2.4	.27	10.9	9,616	.184	1.04	.507	-4.2
112	18.4	61.1	12.5	62.4	11.58	.025	2.5	.29	11.0	9,948	.185	1.04	.497	-4.3
113	18.4	43.7	12.4	45.4	15.85	.027	2.5	.29	10.9	8,731	.258	1.28	.777	-2.8
114	18.4	42.7	12.6	44.5	16.41	.025	2.4	.28	11.2	7,946	.254	1.28	.759	-3.1
115	18.4	34.0	12.5	36.2	20.15	.024	2.4	.28	11.0	7,596	.316	1.51	1.050	-2.0
116	18.4	33.1	12.4	35.3	20.46	.014	2.4	.27	11.0	7,635	.321	1.48	1.105	-1.6
τ = -8°														
117	18.4	84.0	4.9	84.2	3.35	0.118	1.1	0.37	1.7	5,981	0.150	0.38	0.403	-1.6
118	18.4	79.4	10.5	80.1	7.52	.079	2.4	.59	5.6	13,682	.142	.73	.368	-4.4
119	18.4	62.1	12.3	63.3	11.21	.027	2.6	.29	10.9	8,585	.182	.98	.487	-4.3
120	18.4	43.8	12.0	45.4	15.33	.025	2.2	.28	10.8	6,342	.250	1.24	.705	-3.4
121	18.4	34.0	12.1	36.1	19.57	.025	2.2	.27	10.9	5,660	.315	1.48	1.000	-2.1
τ = 0°														
122	18.4	84.0	4.9	84.2	3.32	0.063	1.3	0.24	3.0	4,586	0.130	0.32	0.325	-2.2
123	18.4	84.8	5.0	84.9	3.35	.071	1.2	.27	3.0	3,710	.138	.35	.340	-2.4
124	18.4	78.4	9.3	79.0	6.74	.058	2.1	.43	6.4	7,680	.146	.64	.391	-3.7
125	18.4	80.0	10.3	80.6	7.32	.055	2.5	.47	7.3	8,697	.142	.73	.370	-4.4
126	18.4	78.4	10.4	79.1	7.55	.055	2.5	.47	7.4	8,913	.138	.72	.361	-4.5
127	18.4	74.1	10.0	74.8	7.70	.057	2.3	.46	7.1	8,106	.152	.70	.389	-4.2
128	18.4	73.0	10.0	73.7	7.84	.058	2.4	.45	6.8	8,678	.142	.66	.365	-4.4
129	18.4	73.5	12.1	74.5	9.38	.061	2.8	.57	7.9	11,053	.149	.83	.384	-5.5
130	18.4	61.4	12.1	62.5	11.19	.057	2.4	.56	8.9	9,219	.184	.98	.489	-4.4
131	18.4	61.7	12.2	62.9	11.20	.063	2.6	.60	8.4	10,247	.178	.99	.485	-4.1
132	18.4	60.6	12.2	61.8	11.40	.058	2.6	.60	8.8	9,348	.186	1.01	.487	-4.5
133	18.4	60.4	12.2	61.6	11.43	.059	2.6	.58	8.7	9,841	.172	.98	.471	-4.5
134	18.4	45.2	12.2	46.8	15.14	.057	2.1	.60	9.4	7,501	.238	1.27	.674	-3.6
135	18.4	43.2	12.4	44.9	16.03	.058	2.1	.61	9.5	7,539	.243	1.29	.691	-3.4
136	18.4	42.6	12.4	44.3	16.30	.056	2.0	.62	9.4	7,166	.246	1.28	.719	-3.3
137	18.4	38.8	12.3	40.7	17.62	.058	2.0	.57	9.6	8,091	.275	1.30	.816	-2.7
138	18.4	38.5	12.3	40.4	17.69	.057	1.9	.59	9.7	6,149	.276	1.37	.809	-2.9
139	18.4	38.8	12.4	40.7	17.74	.056	1.8	.58	10.0	6,853	.280	1.39	.812	-3.0
140	18.4	34.0	12.0	36.1	19.45	.055	1.7	.57	9.8	5,563	.295	1.48	.962	-2.2
141	18.4	33.7	12.3	35.8	20.02	.053	1.7	.61	9.8	6,621	.301	1.55	.965	-2.3
142	18.4	33.1	12.5	35.4	20.73	.054	1.8	.60	10.1	6,217	.301	1.53	.969	-2.2
143	36.3	87.3	5.4	87.5	3.53	.147	.9	.54	2.4	8,135	.209	.59	.522	-2.2
144	36.3	76.9	10.8	77.7	7.99	.083	1.7	.73	7.4	15,204	.213	1.14	.538	-4.9
145	36.3	43.7	12.6	45.5	16.10	.149	1.3	1.38	7.2	13,933	.349	1.94	.992	-3.7
146	36.3	36.3	12.6	38.4	19.19	.150	1.2	1.46	7.7	13,121	.420	2.26	1.335	-2.2

TABLE II.- IMPACT TEST DATA - Continued

(b) Curved-stern configuration - Concluded

Run	$C_{\Delta}$	At contact			At $n_{i\max}$					At $z_{\max}$		At rebound		
		$\dot{x}_0$ , fps	$\dot{z}_0$ , fps	$V_0$ , fps	$\gamma_0$ , deg	t, sec	$n_i$	z, ft	$\dot{z}$ , fps	My, lb-ft	t, sec	z, ft	t, sec	$\dot{z}$ , fps
$\tau = 80$														
147	18.4	84.8	5.0	84.9	3.35	0.071	1.6	0.24	2.4	4,272	0.106	0.26	0.211	-2.6
148	18.4	78.4	9.5	79.0	6.89	.068	2.7	.50	5.6	7,853	.128	.63	.308	-5.2
149	18.4	74.1	9.7	74.7	7.43	.070	2.7	.50	5.6	8,239	.133	.64	.325	-5.2
150	18.4	74.1	9.7	74.7	7.46	.072	2.5	.52	5.6	7,273	.135	.66	.340	-5.0
151	18.4	74.4	9.8	75.0	7.50	.069	2.6	.51	5.7	7,940	.131	.63	.316	-5.4
152	18.4	61.7	12.1	62.9	11.13	.066	2.8	.66	8.1	8,965	.154	.96	.419	-5.5
153	18.4	42.6	12.0	44.2	15.76	.066	2.0	.68	9.0	6,336	.233	1.28	.667	-4.0
154	18.4	39.7	12.4	41.6	17.41	.067	2.0	.67	9.8	6,563	.267	1.43	.757	-3.7
155	18.4	39.5	12.4	41.4	17.44	.063	1.9	.69	9.7	5,952	.265	1.42	.738	-3.8
156	18.4	38.6	12.4	40.6	17.81	.063	1.9	.67	9.8	6,187	.268	1.42	.758	-3.6
157	18.4	35.1	11.6	37.0	18.31	.063	1.6	.66	9.2	4,910	.287	1.49	.877	-2.9
$\tau = 160$														
158	18.4	84.0	6.1	84.3	4.17	0.083	2.4	0.32	1.6	5,729	0.093	0.32	0.201	-5.0
159	18.4	74.1	9.9	74.7	7.63	.082	2.9	.57	4.4	7,062	.120	.64	.277	-6.8
160	18.4	73.5	10.2	74.2	7.91	.082	3.0	.57	4.5	6,866	.121	.63	.279	-6.9
161	18.4	73.0	10.3	73.7	8.04	.078	2.9	.58	5.0	7,609	.121	.65	.288	-6.7
162	18.4	67.8	10.0	68.5	8.40	.084	2.7	.62	5.0	6,986	.133	.71	.314	-6.5
163	18.4	51.4	11.4	52.7	12.55	.084	2.2	.75	7.0	6,278	.187	1.04	.470	-5.9
164	18.4	42.5	12.1	44.2	15.89	.085	1.9	.84	8.3	5,708	.225	1.30	.598	-5.1
165	18.4	39.1	12.6	41.0	17.84	.081	1.9	.85	9.0	5,953	.239	1.44	.659	-5.2
166	18.4	39.2	12.6	41.2	17.84	.081	2.0	.84	8.9	6,287	.234	1.39	.634	-5.2
167	18.4	38.8	12.6	40.8	18.03	.082	2.0	.82	9.0	5,955	.237	1.38	.747	-5.1
168	18.4	33.9	12.0	36.0	19.57	.083	1.6	.84	9.0	5,049	.280	1.55	.800	-3.9

TABLE III.- MAXIMUM PRESSURES AND TIME TO PEAK FOR CURVED-UTERN CONFIGURATION

[illegible]

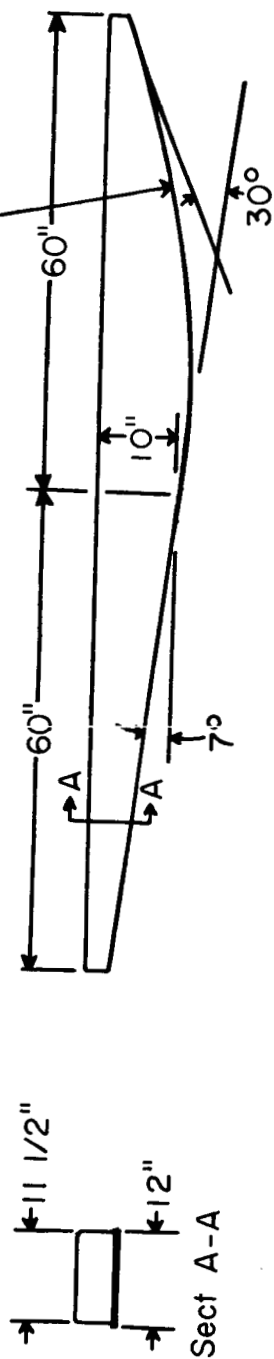
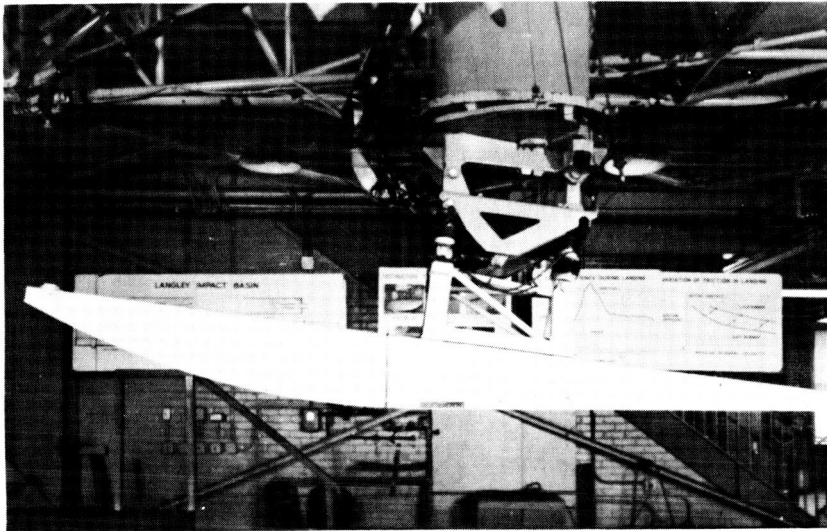


Figure 1.- Profile showing pertinent dimensions of model.

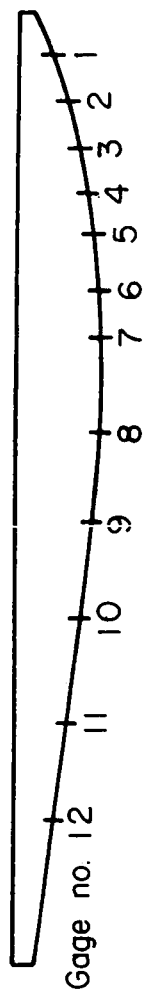


(a) Curved-bow configuration at  $0^\circ$  trim.



(b) Curved-stern configuration at  $0^\circ$  trim. L-59-6464

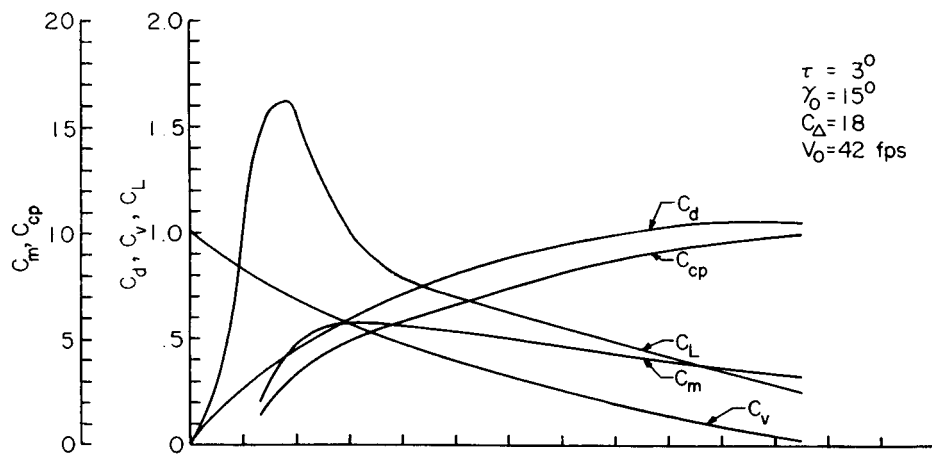
Figure 2.- Photographs of model mounted for testing.



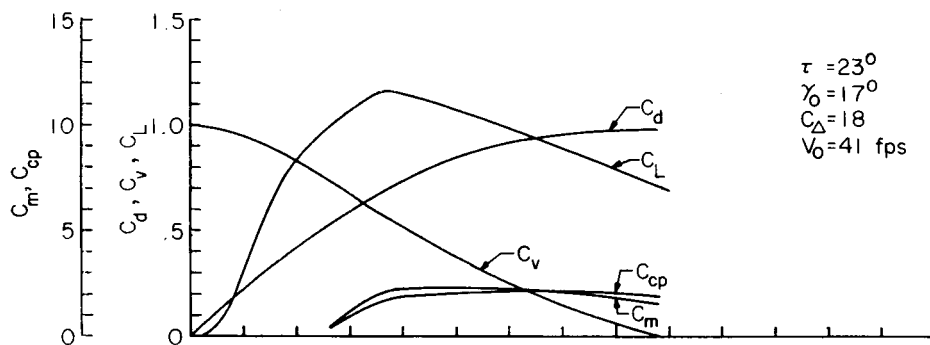
Trim, deg	Draft, feet at pressure gage:											
	1	2	3	4	5	6	7	8	9	10	11	12
16	0.16	0.34	0.54	0.77	0.97	1.29	1.57	2.21	2.87	3.59	4.37	5.11
8	.09	.20	.33	.49	.62	.89	1.12	1.65	2.20	2.82	3.50	4.12
0	.02	.06	.13	.22	.31	.47	.63	1.04	1.48	1.98	2.53	3.03
-8	.04	.01	0	.02	.06	.14	.23	.50	.82	1.19	1.59	2.22
-14	.17	.09	.04	.01	0	.02	.07	.24	.48	.76	1.06	1.34
-22	.53	.38	.26	.15	.09	.03	.01	.03	.15	.29	.45	.59
Distance along bottom from step, ft	0.50	1.00	1.50	2.00	2.42	3.00	3.50	4.50	5.42	6.42	7.50	8.50

Figure 3.- Pressure-gage locations.

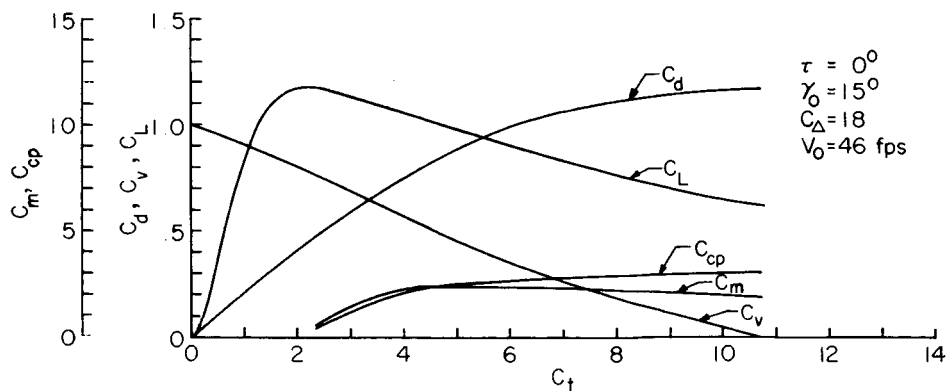




(a) Run 27, curved-bow configuration.

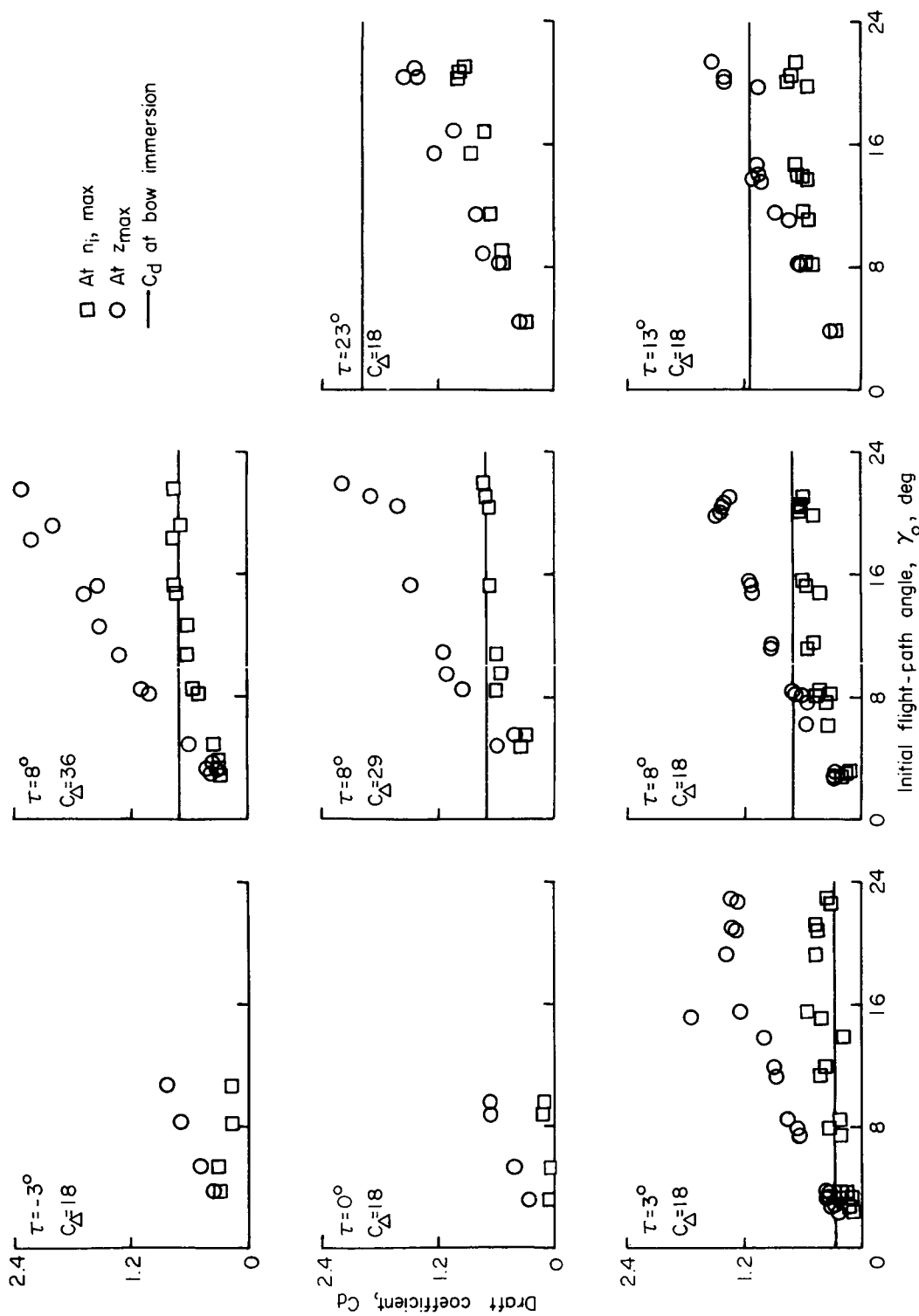


(b) Run 70, curved-bow configuration.



(c) Run 134, curved-stern configuration.

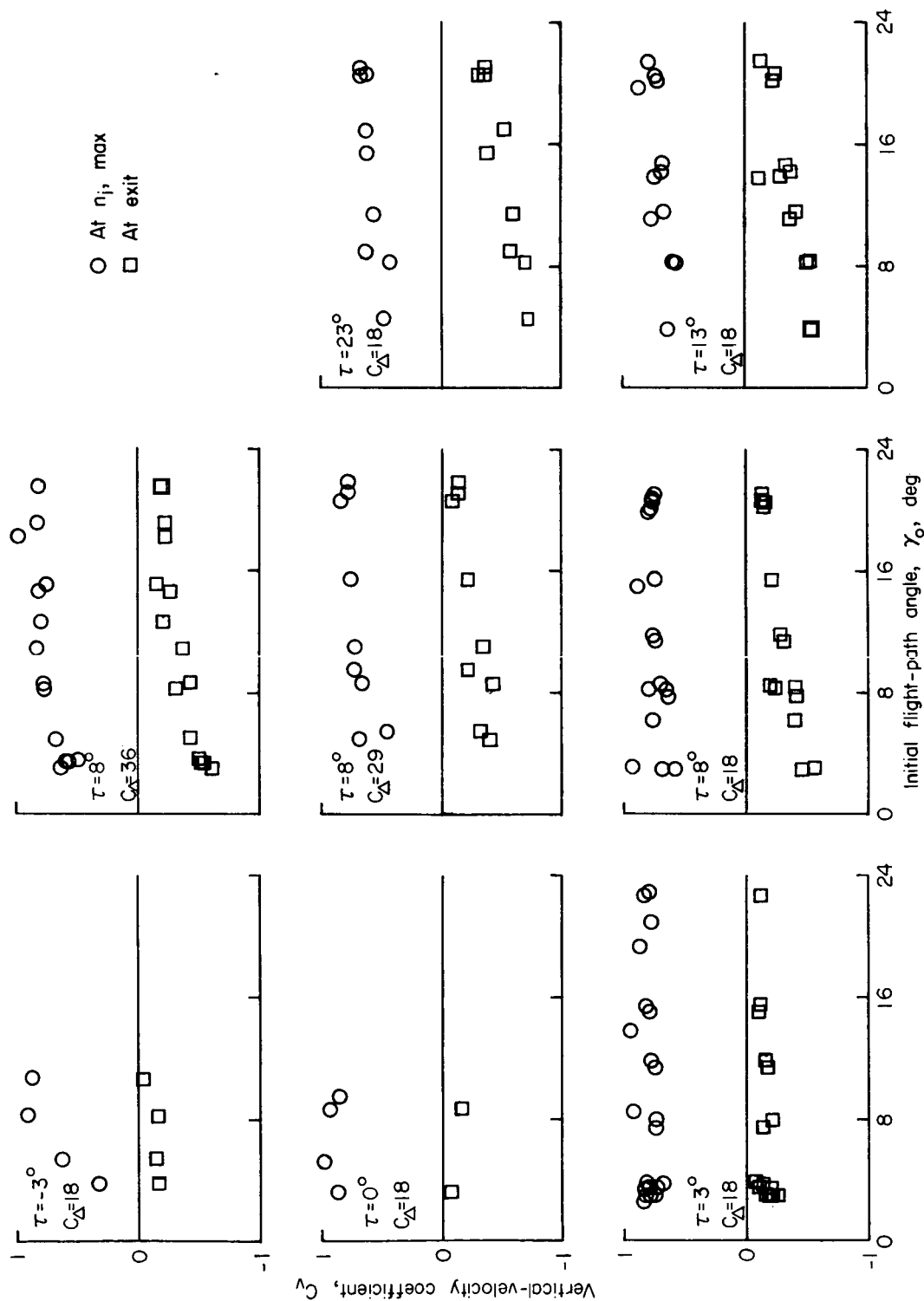
Figure 4.- Time histories of typical runs.



(a) Curved-bow configuration.

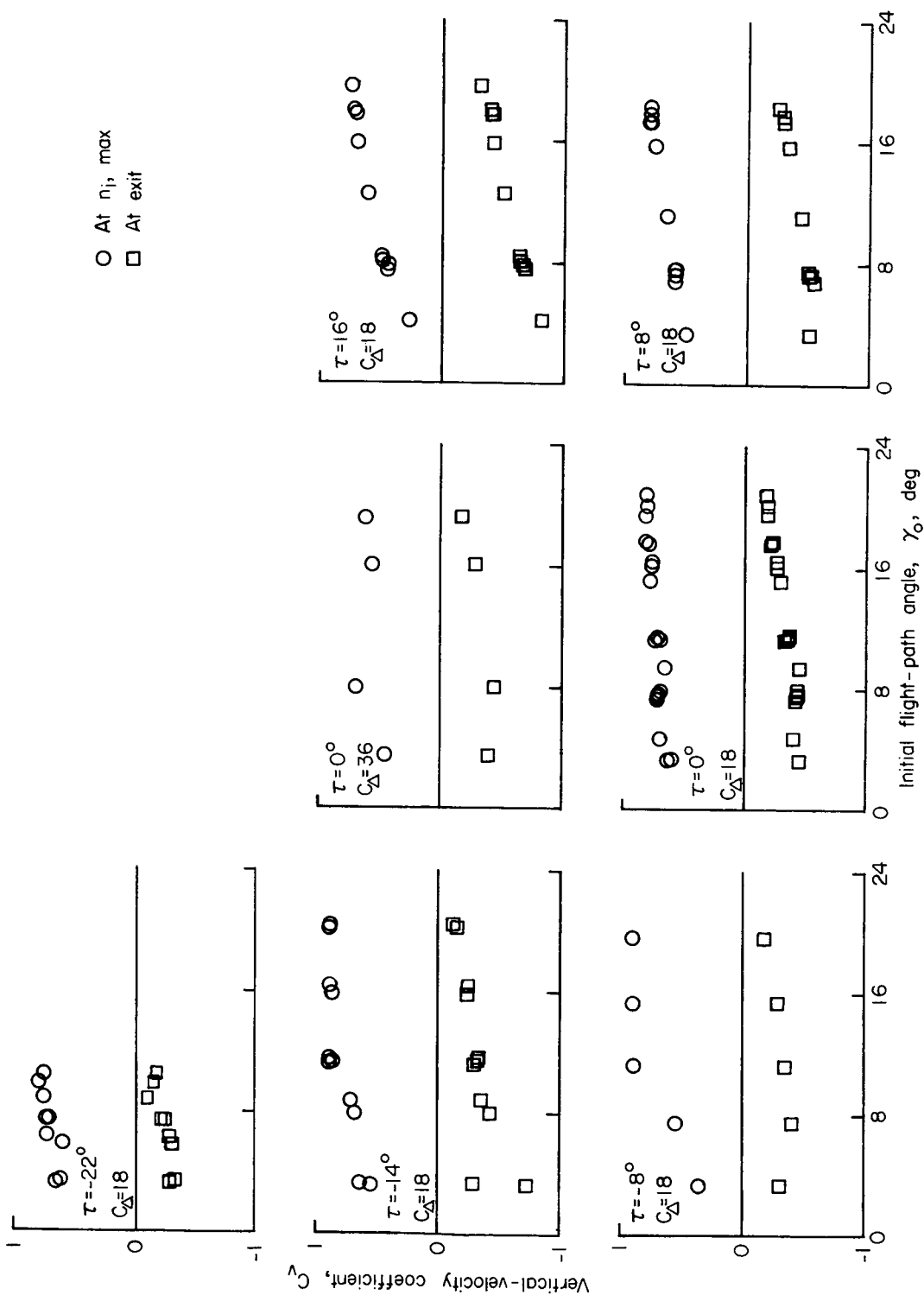
Figure 5.- Experimental variation of draft coefficient with initial flight-path angle.





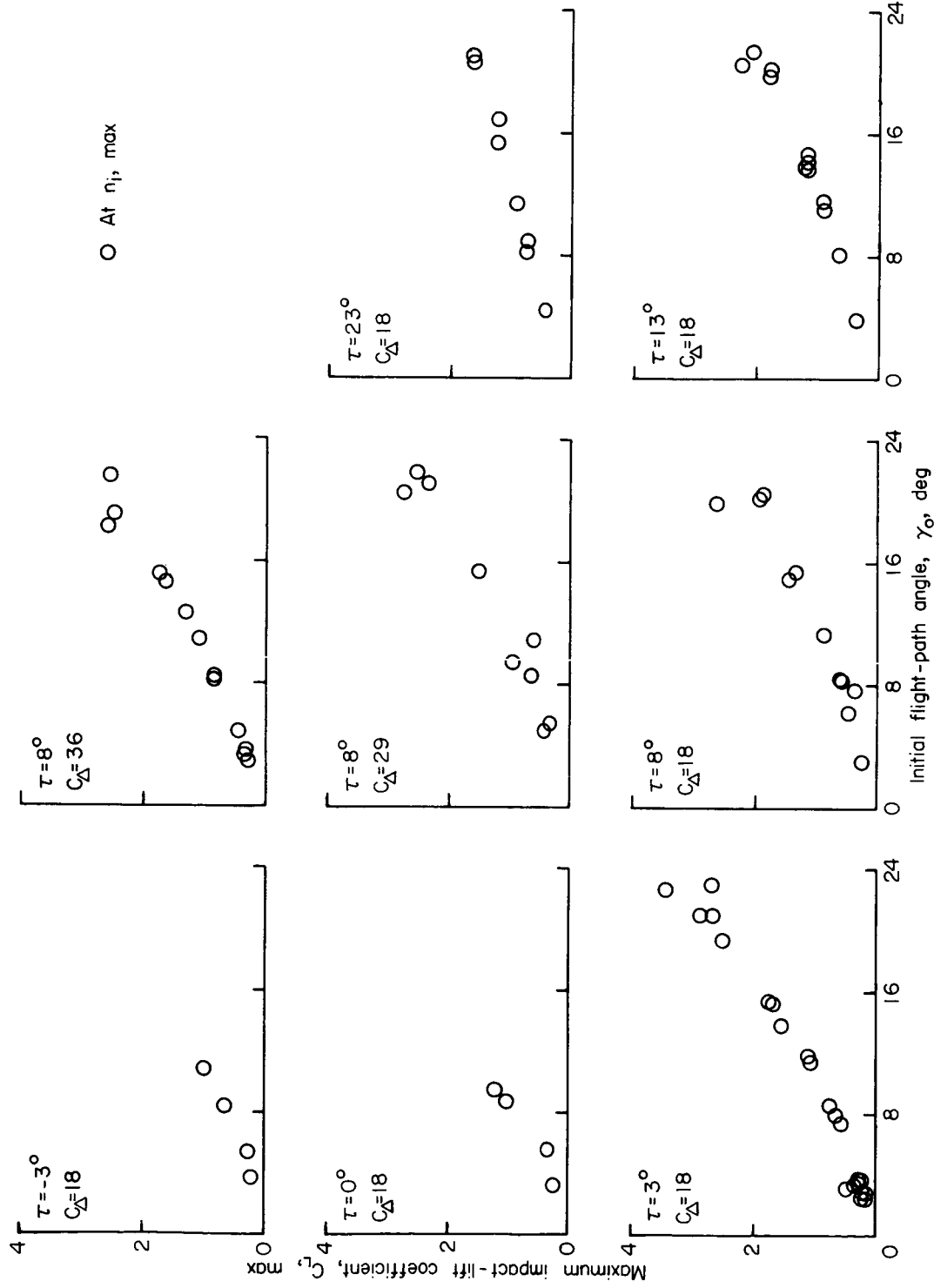
(a) Curved-bow configuration.

Figure 6.- Experimental variation of vertical-velocity coefficient with initial flight-path angle.



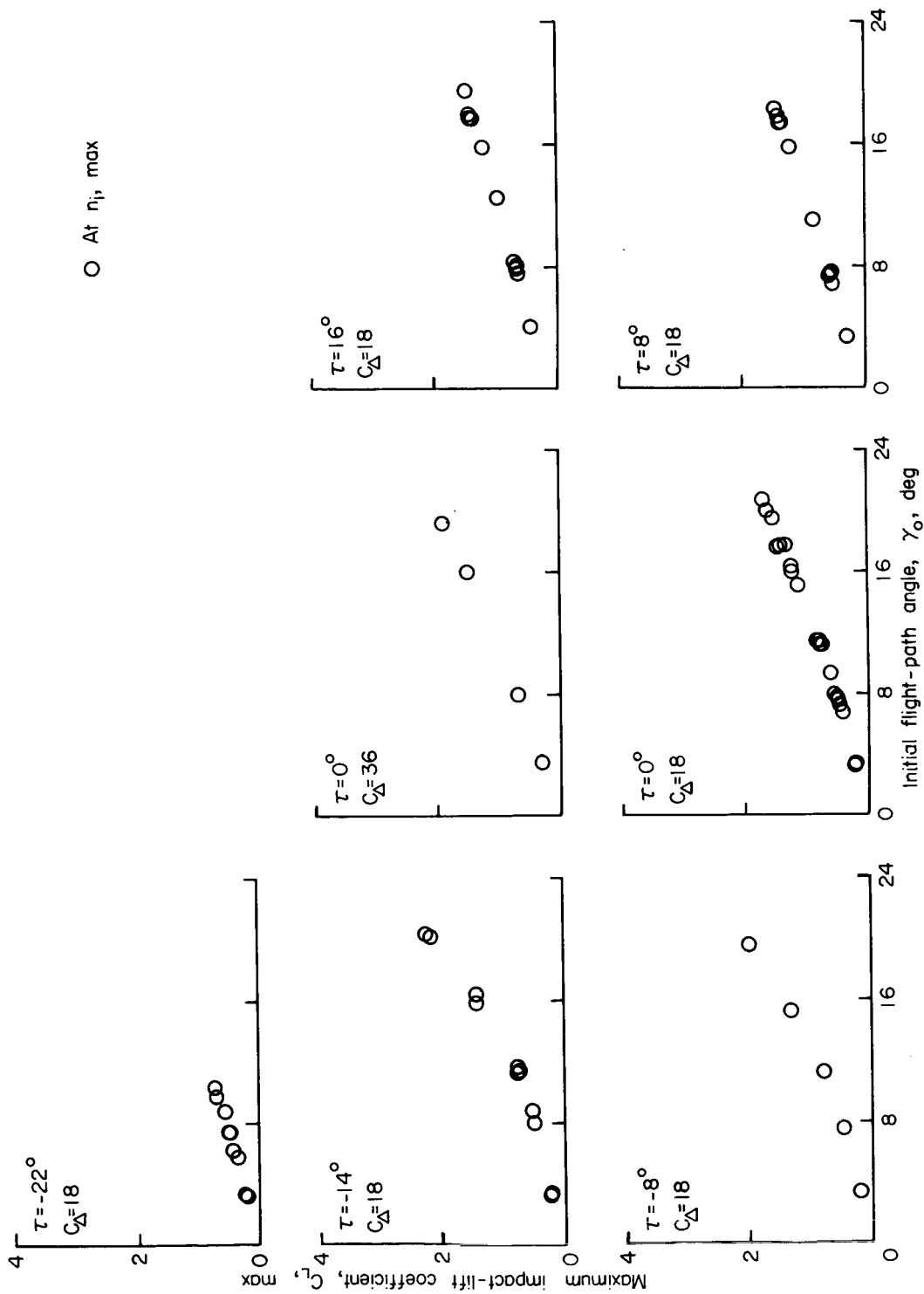
(b) Curved-stern configuration.

Figure 6.- Concluded.



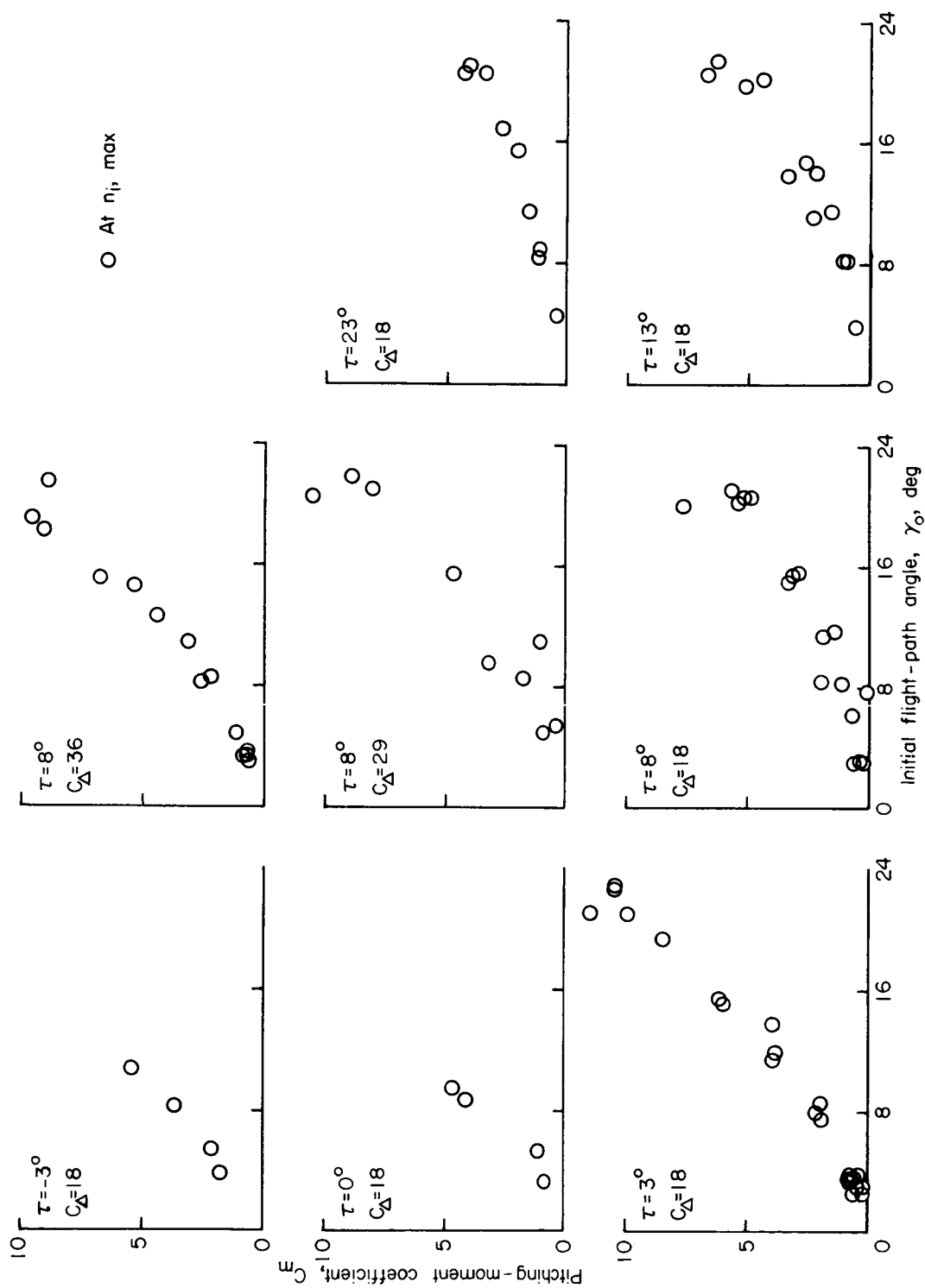
(a) Curved-bow configuration.

Figure 7.- Experimental variation of maximum-impact lift coefficient with initial flight-path angle.



(b) Curved-stern configuration.

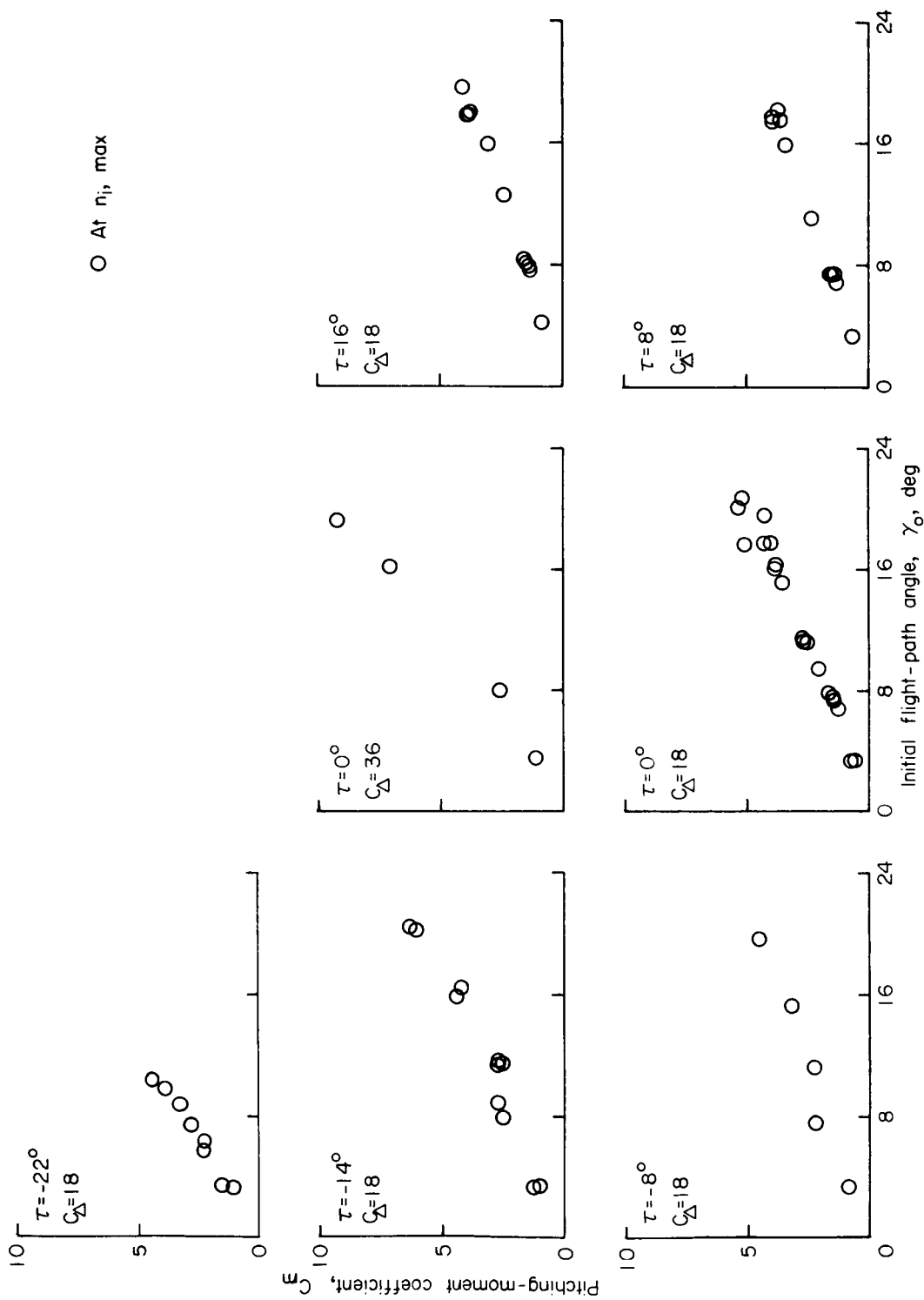
Figure 7.- Concluded.



(a) Curved-bow configuration.

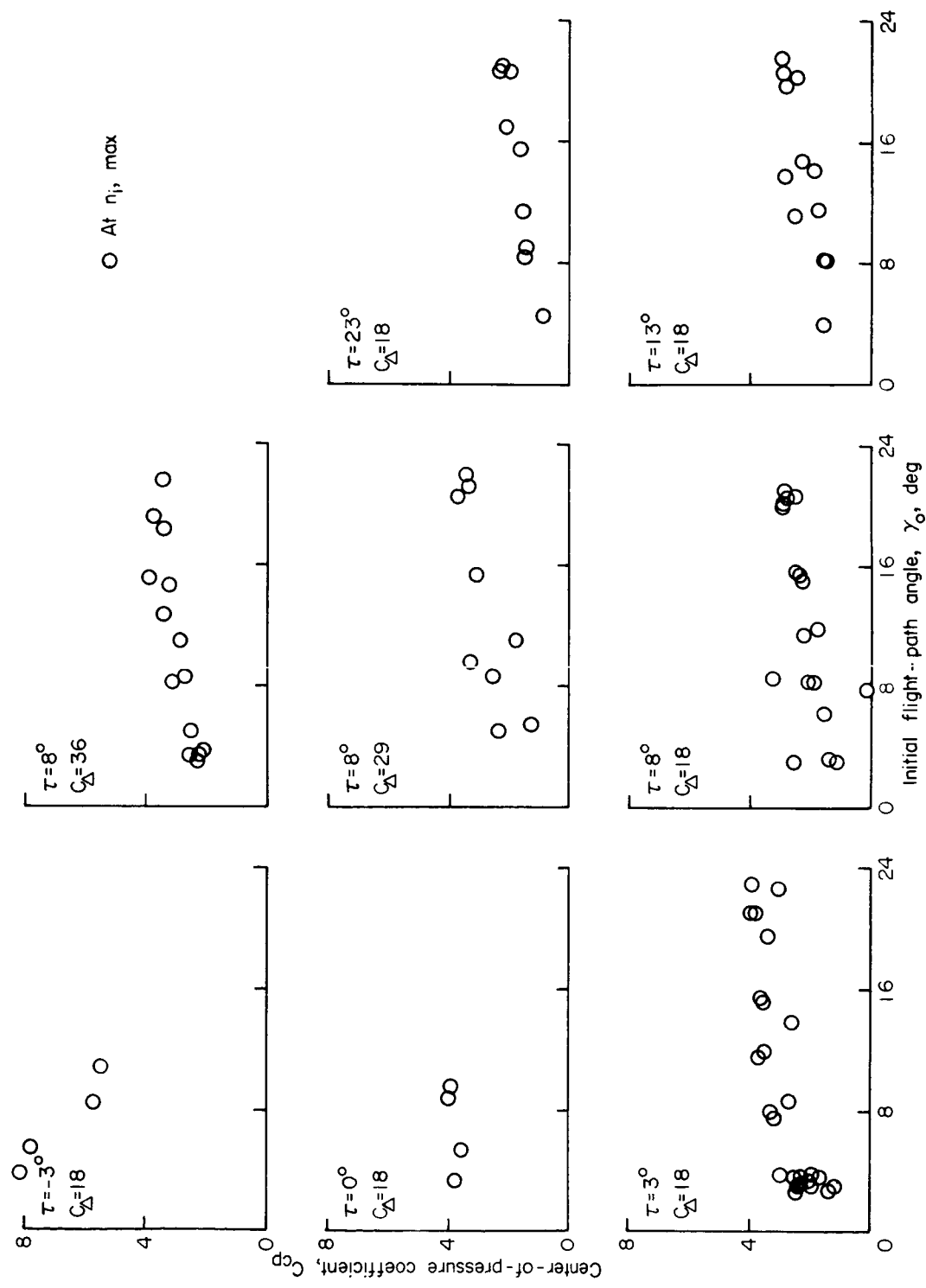
Figure 8.- Experimental variation of pitching-moment coefficient with initial flight-path angle.





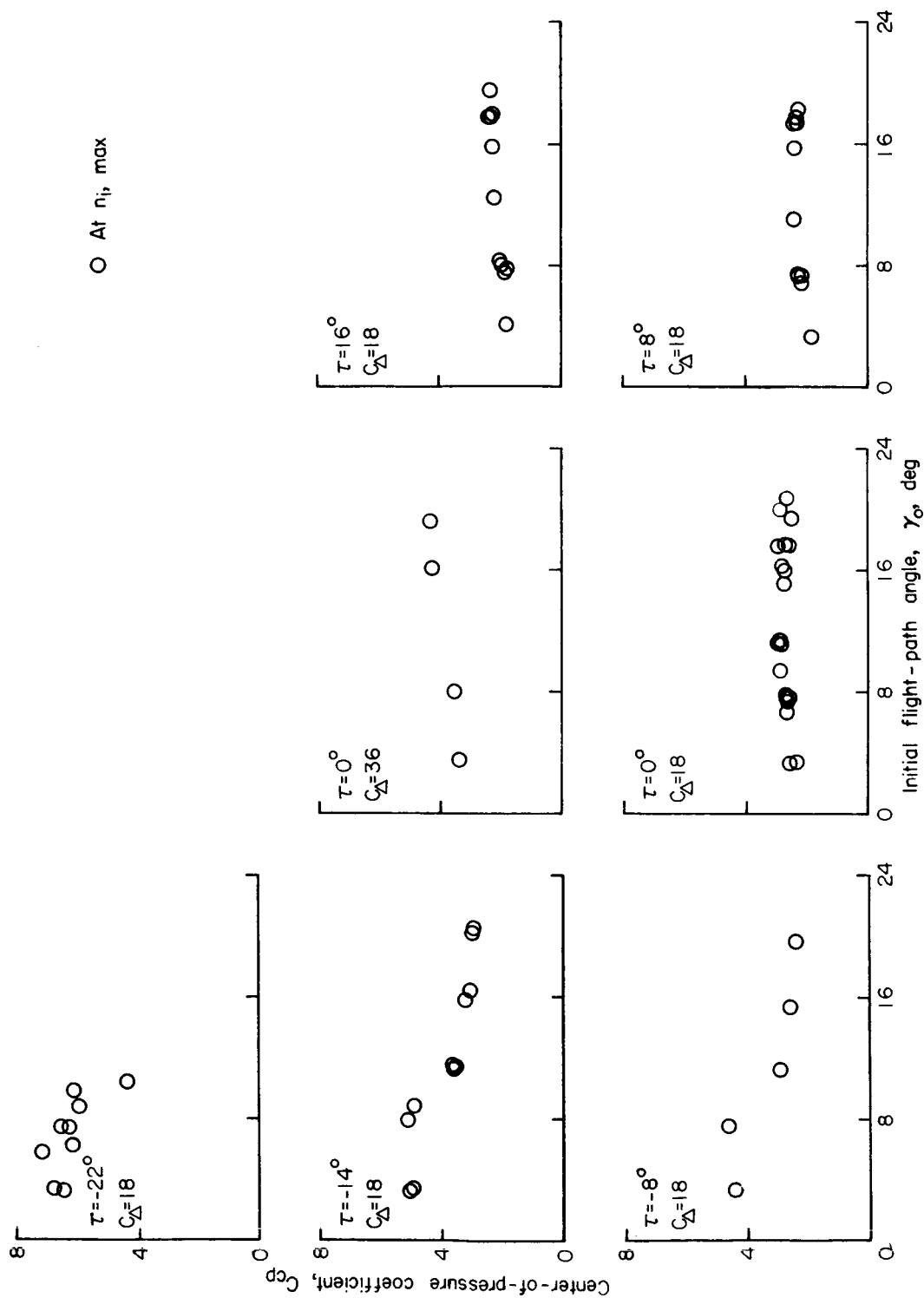
(b) Curved-stern configuration.

Figure 8.- Concluded.



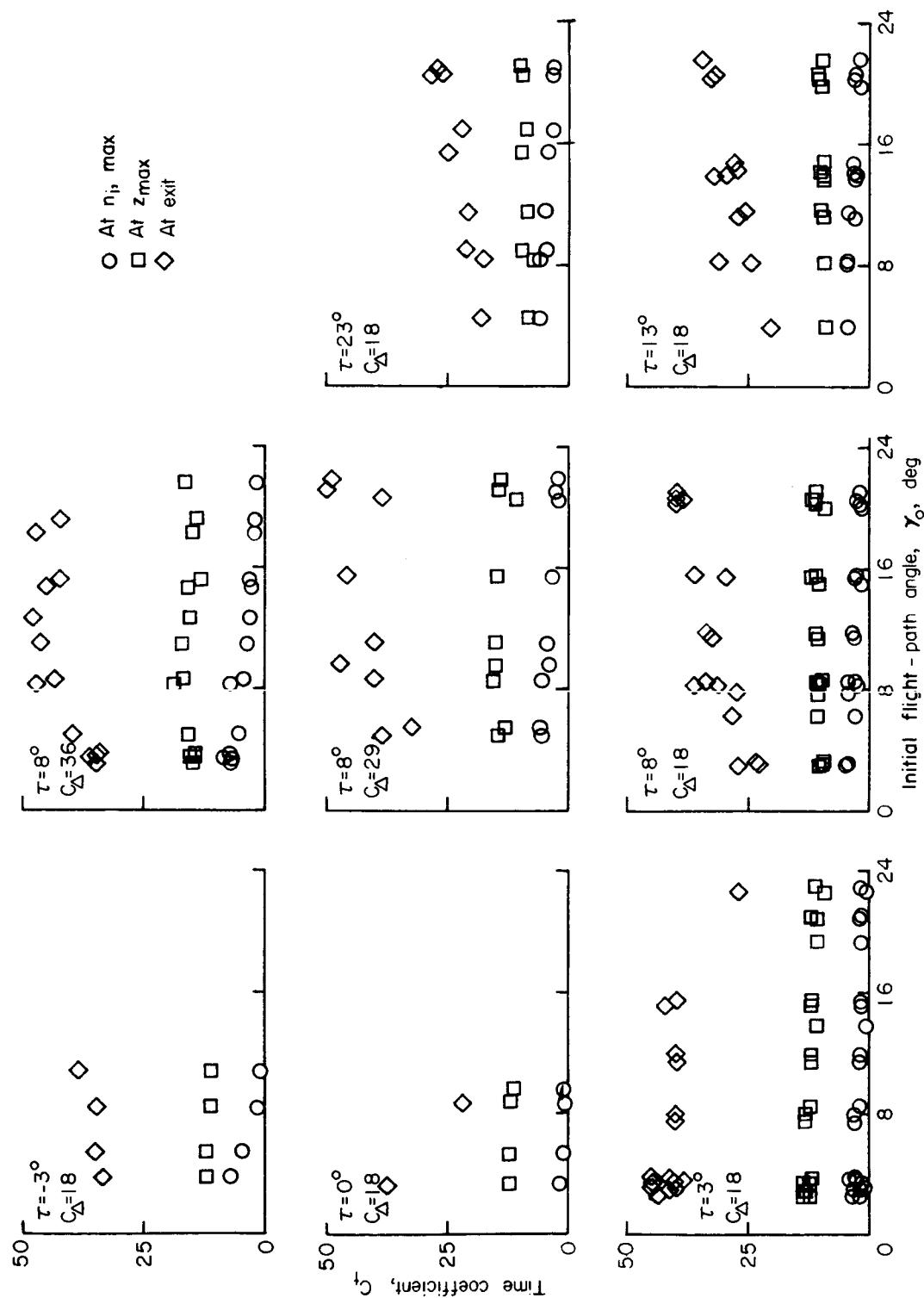
(a) Curved-bow configuration.

Figure 9.- Experimental variation of center-of-pressure coefficient with initial flight-path angle.



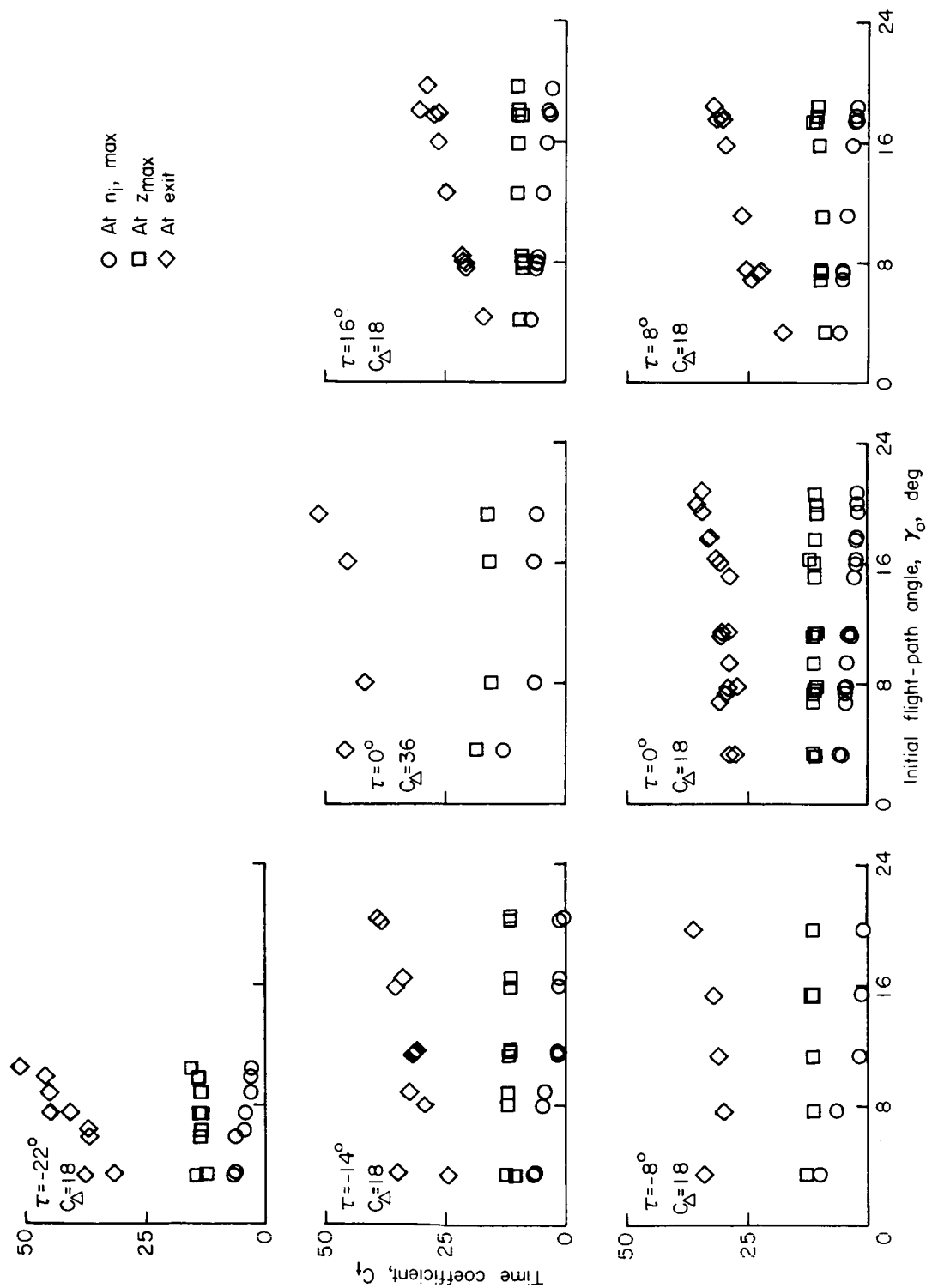
(b) Curved-stern configuration.

Figure 9.- Concluded.



(a) Curved-bow configuration.

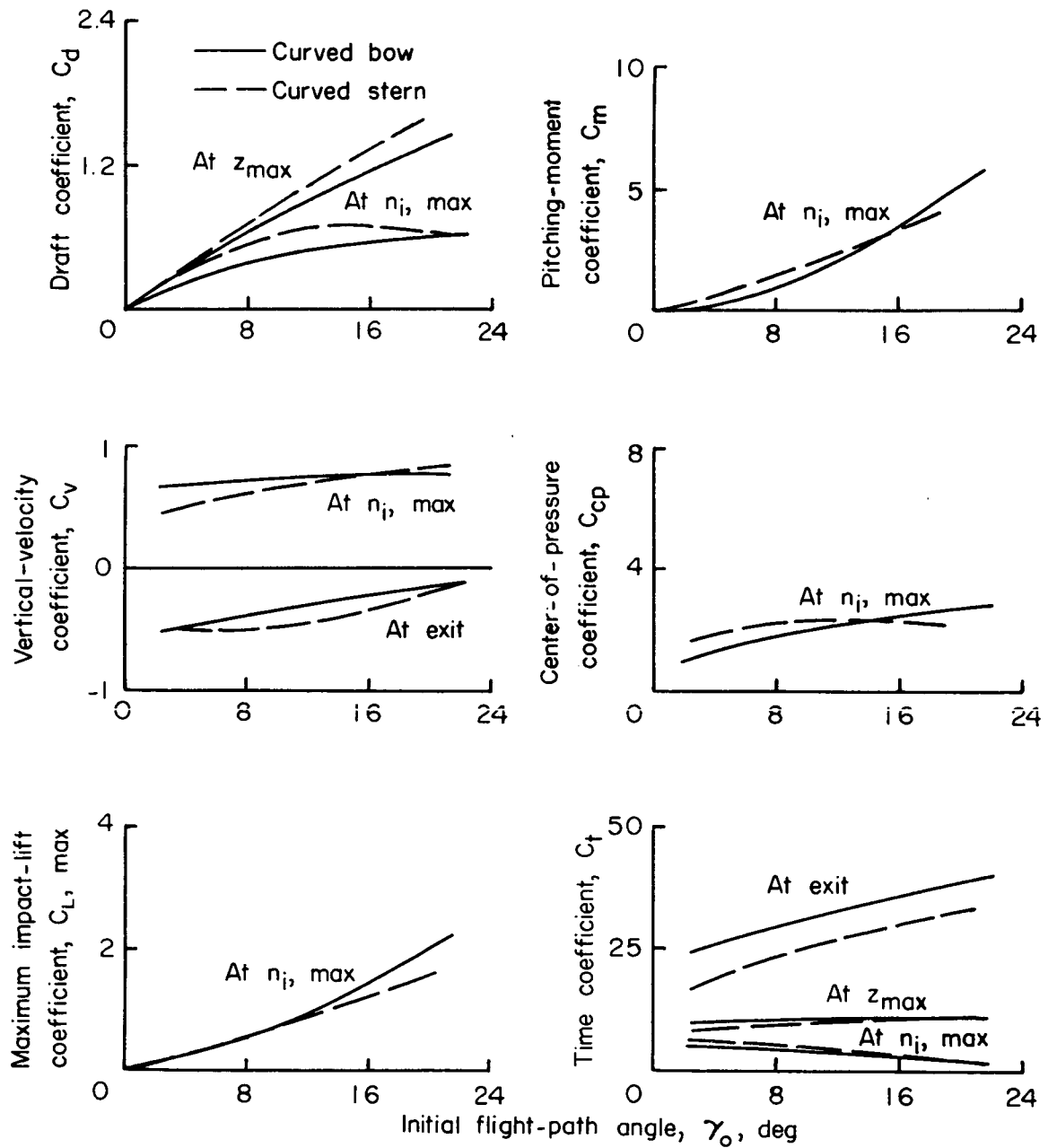
Figure 10.- Variation of time coefficient with initial flight-path angle.



(b) Curved-stern configuration.

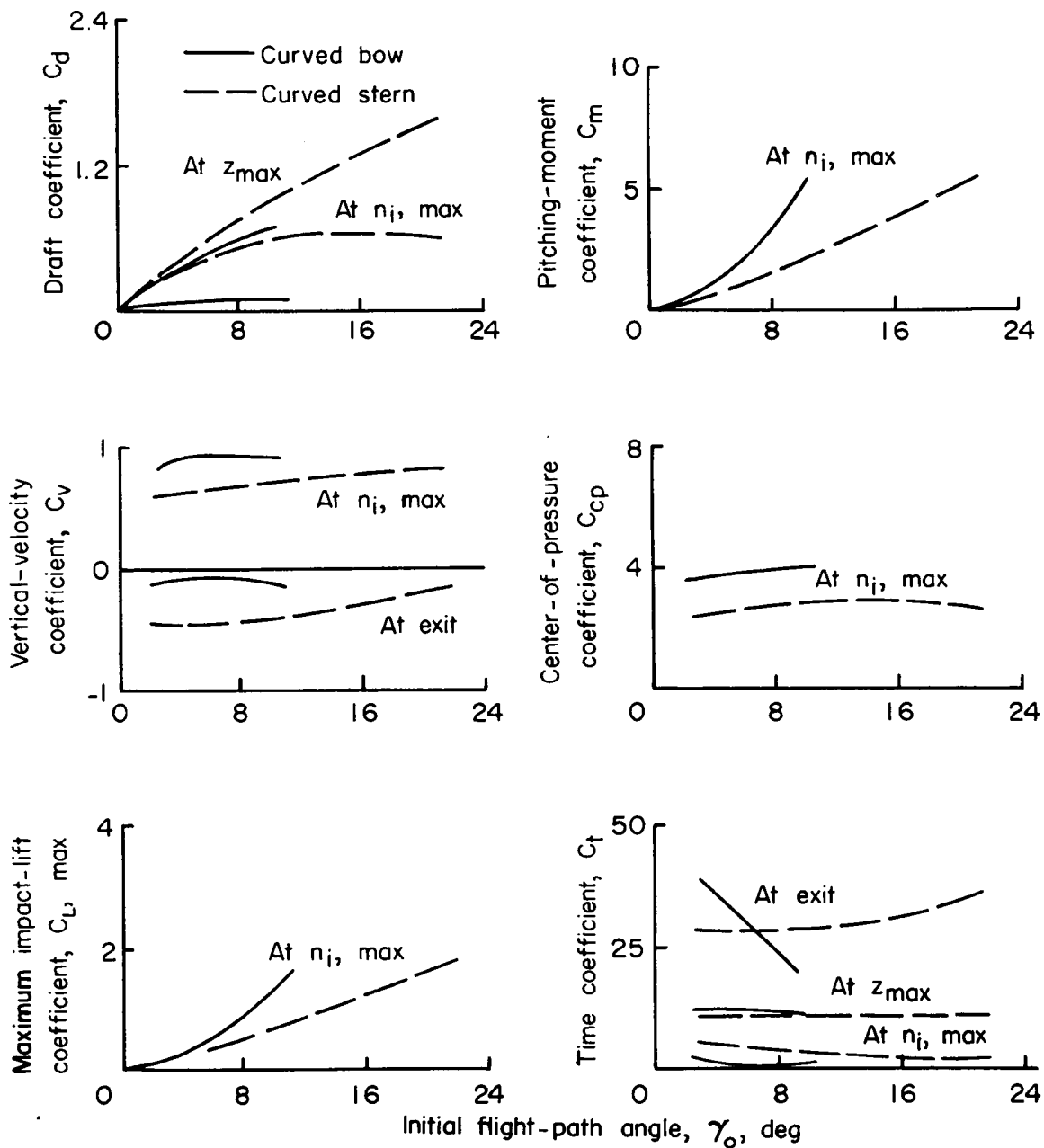
Figure 10.- Concluded.

L-270



(a)  $\tau = 8^\circ$ ;  $C_\Delta = 18$ .

Figure 11.- Comparison of variation of coefficients with initial flight-path angle for curved-bow configuration and curved-stern configuration.



(b)  $\tau = 0^\circ$ ;  $C_\Delta = 18$ .

Figure 11.- Concluded.